NACA

RESEARCH MEMORANDUM

FREE-JET INVESTIGATION OF A 16-INCH RAM JET AT MACH NUMBERS OF 1.35, 1.50, and 1.73

By Fred Wilcox, Sol Baker, and Eugene Perchonok

Lewis Flight Propulsion Laboratory
Cleveland, Ohio

NATIONAL ADVISORY COMMITTEE
FOR AERONAUTICS

WASHINGTON
October 2, 1950

NACA RM E50G19

1

1376

NATIONAL ADVISORY COMMITTEE FOR AERONAUTICS

RESEARCH MEMORANDUM

FREE-JET INVESTIGATION OF A 16-INCH RAM JET AT MACH NUMBERS OF 1.35, 1.50, AND 1.73

By Fred Wilcox, Sol Baker
and Eugene Perchonok

SUMMARY

The results of a free-jet investigation conducted in the NACA Lewis altitude wind tunnel to determine the internal performance of a 16-inch ram jet are presented and discussed. Data were obtained at altitudes between 30,000 and 41,000 feet and at Mach numbers of 1.35, 1.50, and 1.73. A single-oblique-shock spike diffuser with no internal contraction was employed. Special features of the engine were remotely adjustable spike-tip projection, fuel-injector radial position, and exit-nozzle outlet area.

Two flame holders were investigated and both indicated a marked dependence on the radial position of the fuel injector for satisfactory operation. Under conditions of low pressure in the combustion chamber, a blend by volume of 50-percent gasoline and 50-percent propylene oxide appeared to be a superior fuel to gasoline alone.

The best over-all performance from the standpoint of thrust coefficient and thrust specific fuel consumption did not always occur at the largest nozzle-outlet area and the maximum fuel-air ratio at which the engine could be operated. The peak thrust coefficients and the minimum thrust specific fuel consumptions, which were not obtained at the same fuel-air ratios, for each Mach number were

Mach number	Maximum thrust coefficient	Minimum thrust specific fuel consumption lb/(hr)(lb thrust)
1.35	0.61	3.3
1.50	.64	3.2
1.73	.67	3.2

Although subcritical pulsing of low amplitude was encountered, little effect on diffuser pressure recovery was observed. Similar pressure recoveries were obtained under cold-flow and burning conditions. Close agreement was obtained between the frequencies determined from high-speed motion pictures of the shock movement and from instantaneous records of the static pressure at the combustion-chamber inlet.

INTRODUCTION

A free-jet investigation of a 16-inch ram jet with a supersonic inlet has been conducted in the NACA Lewis altitude wind tunnel. Previous ram-jet internal-flow studies in this facility were made by the connected-pipe technique described in references 1 to 3, and on engines having only a subsonic diffuser. The free-jet technique, however, permits investigation of the internal flow through the complete engine at conditions closely simulating free flight.

Engine performance at zero angle of attack was investigated at altitudes from 30,000 to 41,000 feet and at Mach numbers of 1.35, 1.50, and 1.73. Data were obtained with two fuels, gasoline and a blend by volume of 50-percent gasoline and 50-percent propylene oxide. Diffuser, combustion-chamber, and over-all engine performances are presented for the two burner configurations investigated. Representative shadowgraph still and high-speed motion pictures of the air flow about the engine inlet are also included.

APPARATUS

A schematic layout of the altitude-wind-tunnel free-jet facility and a photograph of the 16-inch ram-jet installation are shown in figures 1 and 2, respectively. Air is drawn in from the atmosphere at essentially sea-level pressure, directed through an air dryer to lower the dew point (preventing condensation in the supersonic nozzle), and then through an air heater to raise the air temperature to the stagnation temperature of the simulated flight condition. A throttle valve in the air line is used to set the proper pressure ratio across the supersonic nozzle.

Three supersonic nozzles were employed in this investigation, each with an outlet diameter of 12 inches. On the basis of preliminary surveys of the free-jet flow, the following engine locations were selected:

Jet Mach number	Distance from nozzle outlet to diffuser lip (in.)
1.35	20
1.50	14
1.73	6

The ram jet was mounted above a wing spanning the tunnel test section and exhausted directly into the wind tunnel. A schematic diagram of the engine is shown in figure 3 and the engine coordinates are given in table I. The diameter of the combustion chamber is 16 inches and the over-all engine length is 181 inches, 90 inches of which are combustion chamber and nozzle. A single-oblique-shock spike diffuser designed for external compression was used. The spike (46° included cone angle) was positioned axially by remote control.

The diffuser was made of mild steel, whereas the water-cooled combustion chamber and the nozzle sections were constructed of Inconel.

Fuel was injected at a station upstream of the flame holder through injectors whose radial position could be varied during engine operation. The mechanism (shown in fig. 4) by means of which this adjustment was accomplished was housed in the center body.

A vortex pilot, built into the downstream end of the diffuser center body and similar to that used with the engine described in reference 3, provided a continuous source of ignition. Air entered duct inlets in two of the center-body rear support struts and was discharged into the pilot chamber. Propylene oxide was introduced through a single commercial spray nozzle and the air-fuel mixture ignited with a standard turbojet spark plug.

A water-cooled plug (described in reference 5) that could be moved axially during engine operation was used in conjunction with a converging 13.75-inch-diameter outlet nozzle and gave a variation in nozzle-outlet area of 51 to 74 percent of the combustion-chamber area. (At all plug positions the minimum area was at the nozzle outlet.)

Two different fuel injectors were investigated: the orifice injector (fig. 5), and the spray-nozzle injector (fig. 6). Basically, both injectors consist of four 1/4-inch tubes bent to arc

segments of 6-inch radius and attached to the ends of four radially adjustable supply lines. Each segment of the orifice injector had a total of 25 equally spaced number 70 drill orifices. Every third orifice injected radially inward and the others were directed upstream. Each spray-nozzle injector segment was fitted with four threaded adapters into which were screwed commercial spray nozzles rated at 21 gallons per hour at 100 pounds per square inch fuel pressure. The nozzles were modified externally to reduce their frontal area, and their spray was directed upstream.

Except when otherwise noted, the data presented were obtained with the orifice injector.

The flame holders investigated were the rake (fig. 7), and the serrated annular baffle (fig. 8), which were located 17 inches downstream of the fuel injector. Connected-pipe results previously obtained with these burner configurations are reported in reference 4.

In order to obtain diffuser performance under cold-flow conditions, the momentum pressure drop due to combustion was simulated by substituting an orifice plate for the exhaust nozzle. By positioning the nozzle plug, the mass air flow through the engine could be varied from approximately zero to the critical value.

Observations of the flow about the engine inlet were made with the shadowgraph system sketched in figure 9. Both high-speed motion pictures and still pictures were taken.

The fluctuation of the total and static pressures at station x (fig. 3) was determined with a commercial strain-gage-type pressure pickup. The output of the pickup was amplified and permanently recorded on a strip chart.

Two fuels were used in this investigation: gasoline (AN-F-48b), and a mixture by volume of 50-percent gasoline and 50-percent propylene oxide. In both cases the fuel flow was measured with a rotameter. Except where otherwise noted, the data reported are for gasoline.

PROCEDURE

Inasmuch as the total-pressure loss across the free-jet nozzle was negligible, it was assumed that the pressure recovery across the supersonic portion of the diffuser could be evaluated from total-pressure measurements at the nozzle inlet and at station y (fig. 3) in the engine. The subsonic-diffuser pressure recovery and the

[redacted]

air flow through the engine were evaluated from additional pressure measurements at stations 3 and x, respectively. Jet thrust was calculated from tail-rake pressure data, the accuracy of which was checked by the tunnel scales during the connected-pipe phase of this investigation (reference 4). The calculation methods employed are outlined in references 1 and 2. No evaluation was made of external drag resulting from air spillage around the inlet. Static orifices were located along the spike, the diffuser center body, the outer body of the diffuser, and the combustion chamber.

Combustion efficiency values quoted are based on the enthalpy rise in the gas flowing through the engine plus the heat lost to cooling water as compared with the energy input based on the lower heating value of the fuel.

The values of combustion-chamber-inlet velocity and Mach number are based on the annular combustion-chamber-inlet area, which is approximately 87 percent of the engine frontal area. The net-thrust coefficient is based on an engine frontal area 16 inches in diameter.

Free-stream Mach numbers were computed from the angle of the oblique shock generated by the spike. The pressure ratio required across the free-jet nozzle was obtained by first setting the test-section altitude at the desired value and then adjusting the total pressure at the nozzle inlet to the proper value.

Burning was initiated by first reducing the engine outlet area to the minimum value and igniting the pilot fuel. The main fuel supply was then introduced and the outlet area increased to the desired value. Pilot burning was maintained during engine operation with the spark off at a fuel flow of 12.5 gallons per hour. Under extreme conditions where it was not possible to light the pilot and then the burner by the method described, it was necessary to ignite the engine before setting up the desired pressure ratio across the free-jet nozzle.

At each of the three free-stream Mach numbers and in some cases at several altitudes for the same free-stream Mach number, the fuel-air ratio range and blow-out limits were determined at several engine-outlet areas. The total temperature of the free-jet was adjusted to correspond to the test altitude and free-stream Mach number. At each free-stream Mach number, the spike was positioned to cause the oblique shock it generated to intercept the lip of the inlet at the design condition. Data were also obtained with the spike at off-design positions.

At each fuel-air ratio, the injector position that resulted in the lowest combustion-chamber-inlet Mach number was considered optimum, because it gave the highest value of combustion-chamber temperature ratio. This optimum radial fuel-injector position was selected for each burner configuration and held fixed over most of the operable fuel-air ratio range. Where the blow-out limits could be extended by changing the fuel-injection radius, the results are reported. In general, the same fuel-injection radius was optimum over most of the operable range.

SYMBOLS

The following symbols are used in this report:

A	cross-sectional area, square feet
C_F	net thrust coefficient, $\frac{2F_n}{\gamma_0 p_0 A_4 M_0^2}$
E	equivalence ratio, ratio of actual f/a to stoichiometric f/a
F_n	net thrust, pounds
f/a	fuel-air ratio
M	Mach number
P	total pressure, pounds per square foot absolute
p	static pressure, pounds per square foot absolute
t	static temperature, $^{\circ}F$
W_f/F_n	net thrust specific fuel consumption, pounds fuel per hour per pound of thrust
γ	ratio of specific heat at constant pressure to specific heat at constant volume

η_b combustion efficiency, percent

τ ratio of absolute total temperature at exhaust-nozzle outlet to absolute total temperature at combustion-chamber inlet

Subscripts (refer to fig. 3):

0 free-stream condition

1 supersonic-diffuser inlet

2 subsonic-diffuser inlet (by definition)

3 diffuser outlet and combustion-chamber inlet

4 combustion chamber

5 combustion-chamber outlet

6 nozzle outlet

s spike

x air-flow measuring station

y survey station for subsonic diffuser inlet

RESULTS AND DISCUSSION

Over the range of combustion-chamber-inlet Mach numbers investigated, the total-pressure losses across the rake and serrated annular baffle flame holders were 1.5 and 2.25 times the combustion-chamber-inlet dynamic pressure, respectively.

Rake Flame Holder

Performance at Mach number of 1.35 and altitude of 30,000 feet. - Engine performance with the rake flame holder is presented in figure 10 and is summarized in table II. At M_0=1.35 (fig. 10(a)), the tunnel pressure altitude was set at 30,000 feet and the jet total temperature was adjusted to 100° ±10° F. At fuel-air ratios richer than 0.045, the data were obtained with a fuel-injection radius of 5.94 inches. In order to operate at fuel-air ratios leaner than 0.045, the fuel-injection radius was reduced to 5.62 inches.

[redacted]

Results are presented for outlet-area ratios A_6/A_4 of 0.739, 0.676, 0.650, and 0.600. The inlet operated in the subcritical region at all times, and resulted in a combined subsonic and supersonic diffuser total-pressure recovery between 97 and 98 percent.

As expected, the combustion-chamber-inlet Mach number M_3 rose as the engine-outlet area was increased. Over the range of fuel-air ratio f/a and A_6/A_4 investigated, however, the variation was small enough that the combustion-chamber-inlet static pressure p_3 remained relatively constant at 1770 ±10 pounds per square foot absolute. The effect of outlet area on gas total-temperature ratio τ, thrust coefficient C_F, combustion efficiency η_b, and specific fuel consumption W_f/F_n, however, is more complex. Although the operable f/a range of 0.041 to 0.076 was essentially the same for all four outlet-area ratios, the largest A_6/A_4 of 0.739 gave lowest values of combustion efficiency due to the higher M_3 values. At the other three outlet-area ratios, the combustion efficiencies were approximately the same for fuel-air ratios below 0.052. At richer values, however, the combustion efficiency fell slightly as the nozzle-outlet area was progressively increased.

Between fuel-air ratios of 0.041 and 0.060, the combustion efficiency with each outlet area was relatively constant. Combustion efficiency decreased at richer values with a corresponding leveling off and decrease in the value of τ. Peak combustion efficiencies were in the order of 78 percent (M_3=0.17) and peak τ values, 5.8.

Although the maximum τ was attained with the smallest outlet-area ratio A_6/A_4 = 0.600, the low mass air flow through the engine with this outlet area gave thrust coefficients C_F below those resulting with the larger outlet areas. The thrust coefficients obtained with the three large outlet areas differed only slightly. The maximum value of C_F was 0.61 and occurred near the stoichiometric fuel-air mixture. Increases in f/a to rich blow-out resulted in no change in C_F, whereas decreases in f/a below stoichiometric were accompanied by a gradual reduction in C_F.

The thrust specific fuel consumption W_f/F_n increased, in general, with f/a and outlet area. Near the maximum thrust coefficient C_F = 0.60, the minimum W_f/F_n was 4.1 pounds per hour per pound of

thrust and was obtained at $f/a = 0.066$ and $A_6/A_4 = 0.676$. This thrust coefficient could be obtained less economically by operating at a richer f/a or with a larger outlet area. Thus, for maximum thrust at $M_0 = 1.35$ and an altitude of 30,000 feet, the most economical internal engine performance was obtained at an A_6/A_4 and f/a below the maximum values at which the engine could be operated.

The minimum over-all W_f/F_n was 3.3 and occurred with $C_F = 0.52$ at $f/a = 0.041$ and $A_6/A_4 = 0.650$.

Performance at Mach number of 1.50 and altitude of 35,000 feet. - The total temperature of the air was set at $110^\circ \pm 10^\circ$ F. At outlet-area ratios of 0.739, 0.676, and 0.600, data were obtained with a fuel-injection radius of 5.94 inches, whereas at area ratios of 0.550 and 0.512, data were obtained at a fuel injection radius of 6.32 inches. Increasing the injection radius extended the lean blow-out limit (fig. 10(b)). This extension of the lean blow-out limit was accompanied by a sharp drop in the combustion efficiency and a marked rise in W_f/F_n.

Except for conditions at $f/a = 0.033$, which corresponded to critical diffuser operation, all data presented are for operation in the subcritical region. The combined subsonic and supersonic total-pressure recoveries varied between 91 and 93.5 percent, and resulted in combustion-chamber-inlet static pressures between 1620 and 1670 pounds per square foot absolute. As expected, the values of C_F increased with f/a and decreased progressively as the nozzle-outlet area was reduced. The range of inlet Mach numbers over which the combustion chamber was operated extended from 0.133 to 0.201.

Although the maximum combustion efficiencies occurred at and below the stoichiometric mixture, peak values of τ were obtained above the stoichiometric f/a. Minimum thrust specific fuel consumption, however, resulted at fuel-air ratios near 0.05. The complex relation between engine performance and engine configuration is again emphasized by these data. Although essentially the same C_F values are obtained with A_6/A_4 of 0.739 and 0.676, because of higher combustion efficiencies the thrust specific fuel consumptions are lower with the smaller outlet. At the maximum thrust coefficient (C_F=0.64) obtainable with either of these area ratios, the minimum W_f/F_n was 4.3 pounds per hour per pound of thrust. Dropping the

value of C_F to 0.60 by decreasing the fuel-air ratio reduced the value of W_f/F_n to 3.4. This condition occurred at $f/a = 0.056$, $M_3 = 0.162$, $\tau = 5.25$ and $\eta_b = 77$ percent, the peak combustion efficiency. Thus it is obvious that at $M_0 = 1.5$ too, better internal engine performance results with an outlet area less than the maximum at which the engine was investigated.

Performance at Mach number of 1.73 and altitude of 41,000 feet. - Engine performance at a free-jet Mach number of 1.73 was determined at an altitude of 41,000 feet and a free-stream total temperature of $160^\circ \pm 10^\circ$ F (fig. 10(c)). Data are presented for outlet-area ratios of 0.739, 0.676, 0.600, 0.550, and at a fuel-injection radius of 5.94 inches.

Although M_3 differed considerably for the various outlet areas at a given f/a, the spread in η_b was less than 10 percent. As a result of this narrow spread in η_b, the variation in the values of τ as the outlet area was changed is also small.

Diffuser total-pressure recovery is more sensitive to off-design operation at this Mach number than at either 1.35 or 1.50. The peak combined subsonic and supersonic total-pressure recovery was approximately 88 percent, whereas the lowest measured recovery was 85 percent.

Both the thrust coefficient and M_3 increased as the outlet area increased. The maximum thrust coefficient (0.67) was obtained with the largest outlet-area ratio at f/a of 0.065. At this condition, W_f/F_n was 3.7, τ was 4.6, and M_3 was 0.185. A slight decrease in f/a to 0.058 lowered C_F slightly to 0.66 and reduced the thrust specific fuel consumption to 3.5. Both the peak C_F value and the minimum W_f/F_n value (3.2) were obtained with a diffuser pressure recovery of approximately 88 percent.

At this altitude and Mach number, the highest value of C_F was obtained with the largest outlet area investigated and at a value of W_f/F_n not greatly different than with the smaller outlet area.

Performance comparison at Mach numbers of 1.35, 1.50, and 1.73. - Analysis of figure 10 and the tabulated data in table II indicates that the operable fuel-air ratio range was somewhat less at $M_0 = 1.73$ than at either 1.35 or 1.50. Maximum engine performance (from

consideration of both C_F and W_f/F_n) was not always attained at the highest mass-flow rates. Only at $M_0 = 1.73$ did the largest outlet-area ratio investigated (0.739) give maximum engine performance. At $M_0 = 1.35$ and 1.50, maximum engine output and best fuel economy were obtained at $A_6/A_4 = 0.676$, a value less than the maximum investigated.

Operation was obtained over the same M_3 range (0.13-0.20) at all three free-stream Mach numbers (fig. 10). In spite of the decreasing η_b and τ values, the thrust coefficient was raised and the thrust specific fuel consumption lowered as M_0 was increased. These trends were due to the increased cycle efficiency caused by the greater compression available across the engine.

The data at $A_6/A_4 = 0.739$ presented in figure 10 and summarized in table II, have been plotted as a function of M_0 for several values of f/a (fig. 11). The variation in combustion-chamber-inlet static pressure was small (1640 to 1780 pounds per square foot), and its effect on combustion is considered negligible (reference 5). The inlet-air total temperature, however, was increased from 100° to 160° ±10° F as the free-stream Mach number was raised from 1.35 to 1.73. Instead of the beneficial effect on burner performance that might be expected to accompany an inlet-air temperature increase, the f/a range was the narrowest at $M_0 = 1.73$. For the case illustrated, the combustion efficiency decreased only slightly as M_0 was raised. At lower outlet-area ratios, a marked decrease in η_b was observed when M_0 was increased from 1.50 to 1.73. The increase in inlet-air temperature and the decrease in η_b is reflected in the value of τ, which decreased progressively as M_0 was increased.

At all three values of M_0, the experimental supersonic-diffuser total-pressure recovery fell above normal shock recovery but below the theoretical recovery for one oblique shock followed by a normal shock. Part of this difference may be charged to off-design diffuser operation.

Over a range of M_3 from 0.17 to 0.20, the loss in total pressure across the subsonic diffuser remained between 1 to 2 percent at all three free-stream Mach numbers.

Effect of Fuel Injector on Burner Performance

A comparison of the combustion-chamber performance at $M_0 = 1.35$ with the rake flame holder and two different fuel injectors, the spray nozzle (fig. 6) and the orifice injector (fig. 5), is given in figure 12. The data were obtained at $M_0 = 1.35$ with a blend by volume of 50-percent gasoline and 50-percent propylene oxide as fuel. Best operation with the spray-nozzle injector was obtained at a fuel-injection radius of 5.12 inches, whereas with the orifice injector best operation resulted at a fuel-injection radius of 5.94 inches.

Results with the spray-nozzle injector are shown in figure 12(a) at two outlet-area ratios and two altitudes. At an altitude of 35,000 feet and an outlet-area ratio of 0.676, the operable f/a range was from 0.031 to 0.057. (The stoichiometric f/a of 0.081 for the fuel used was well above the rich limit of 0.057.) The peak combustion efficiency of 75.4 percent occurred near the rich blow-out. When the altitude was raised to 40,000 feet, the inlet air was throttled to maintain the same pressure ratio across the supersonic nozzle and p_3 dropped from approximately 1400 pounds per square foot absolute to approximately 1100 pounds per square foot absolute. The operable fuel-air ratio range was reduced at this lowered pressure.

Similar data are presented in figure 12(b) for the orifice injector. For purposes of comparison, the curve at 35,000 feet and an outlet-area ratio of 0.676 for the spray-nozzle injector is also shown. Although the fuel-air-ratio range with the orifice injector was narrower than with the spray-nozzle injector, it extended to richer fuel-air ratios. Inasmuch as the peak combustion efficiency was 81 percent, greater values of η could be obtained with the orifice injector than with the spray-nozzle injector. For operation over a wider range of η, however, the spray-nozzle injector should be used. Similar results were obtained in the connected-pipe phase of the investigation of this engine (reference 4).

Effect of Propylene Oxide on Burner Performance

The effect on burner performance of using as a fuel a 50-percent mixture by volume of gasoline and propylene oxide instead of gasoline alone is summarized in figure 13. The investigation was made

at $M_0 = 1.35$ and with the orifice fuel injector. In order to facilitate comparison between gasoline and the blend, the data are plotted as a function of equivalence ratio E, that is, the ratio of the actual fuel-air ratio to the stoichiometric fuel-air ratio. The stoichiometric f/a is 0.067 for gasoline and 0.081 for the blend.

Although the operable equivalence-ratio range is approximately equal for both fuels, the blend operated at leaner absolute values. The peak combustion efficiency obtained with the blended fuel was 81 percent (E = 0.67), whereas the peak attained with gasoline was only 73 percent (E = 0.81). A maximum τ value of 5.2 was attained with both fuels. At the peak τ, a slightly lower W_f/F_n resulted with the blend (4.0 lb fuel/(hr)(lb thrust)) than with gasoline because of the lower fuel-flow rate required (lower E). At a given value of E, in spite of higher η_b with the blend, however, a lower W_f/F_n could be obtained with gasoline because of its greater heating value (gasoline = 19,000 Btu per pound; blend = 16,060 Btu per pound).

The range of M_3 over which the engine was operated was essentially the same for both fuels. Moreover, it was possible to burn with either fuel at a combustion-chamber-inlet static-pressure level of 1385 ±10 pounds per square foot absolute at a somewhat reduced range of equivalence ratios. At an outlet-area ratio of 0.739, the same η_b resulted with gasoline for $p_3 = 1385$ as for $p_3 = 1750$ pounds per square foot absolute.

Burning was smooth, and the combined subsonic and supersonic pressure recovery over the entire operable range was 96 ±1 percent with either fuel.

The operable range with gasoline presented in figure 13 is somewhat less than previously obtained with the same configuration in a duplicate test (fig. 10(a)). A possible explanation for this difference is an approximate 7-percent greater pilot fuel flow for the data of figure 10(a). An additional cause could be some physical change in the engine, which had been operated for approximately 30 hours between the runs at which these two sets of data were obtained and had been disassembled several times to change flame holders and fuel injectors.

Serrated Annular Baffle Flame Holder

The performance results with the serrated annular baffle flame holder (fig. 8) and the orifice injector at $M_0 = 1.35$, 1.50, and 1.73 are summarized in figure 14. In order to operate the engine at $f/a = 0.0512$ and 0.0546 with an outlet-area ratio of 0.739 (M_0=1.35), a fuel-injection radius of 5.94 inches was required. All other data were obtained at an injection radius of 5.36 inches.

Engine operation with this burner configuration was possible only over a narrow f/a range. Therefore, in view of the limited performance attainable with this configuration, the results obtained are discussed only briefly. The trend previously indicated of the general η_b level decreasing as M_0 was raised is also demonstrated with this burner. Variation in p_3 is not considered sufficient to cause this reduction. The burner was operated over a range of M_3 from 0.143 to 0.189 with the maximum $\eta_b = 79$ percent occurring at $M_3 = 0.161$. Because of reduced η_b and higher inlet-air temperatures, the τ values at $M_0 = 1.73$ are below those obtained at the two lower Mach numbers. As a result, the highest C_F (0.61) occurred at $M_0 = 1.50$, and the low W_f/F_n of 3.4 attained at $M_0 = 1.73$ could also be attained at $M_0 = 1.35$.

Little scatter was obtained in the over-all diffuser pressure-recovery data and, in general, the combustion efficiencies and diffuser pressure recoveries are comparable to values obtained with the rake-type flame holder. An exception is the pressure recovery at $M_0 = 1.73$, which was approximately 3 percent less than the values obtained with the rake flame holder. The engine was operating near blow-out when these data were taken, and inlet shock oscillation was evident. Not only is such a condition usually accompanied by reduced pressure recovery (reference 6), but the accurate determination of a fluctuating pressure with ordinary instrumentation is questionable.

Diffuser Performance

Representative shadowgraph pictures of the air flow about the diffuser inlet for all three free-stream Mach numbers are given in figure 15. These and all other data which follow were obtained using the rake-type flame holder. At each M_0 a typical photograph is shown for cold flow, burning, and pulsing conditions.

[redacted]

From these photographs, the different tip projections required at the three Mach numbers for interception by the lip of the oblique shock generated by the spike are clearly evident. Inasmuch as the engine-inlet diameter was 9 inches and the free-jet discharge diameter only 12 inches, the normal shock present during subcritical operation often extended to the boundary of the free jet. The intersection of the normal shock and the free-jet boundary is indicated on the photographs as a white line. For the outlet areas investigated the burning conditions usually created a level of back pressure that resulted in subcritical flow at the diffuser inlet. Little data were therefore obtained at design or supercritical flow conditions.

The illustrations showing shock pulsations (fig. 15) are representative of the maximum oscillation encountered at each M_0. With the type of diffuser employed on this engine, the total-pressure recovery in the subcritical flow range did not vary greatly from the value attained at design conditions. Under pulsing, the shock movement was usually restricted to the subcritical region, and the pressure recovery was not seriously reduced. In general, a more noticeable effect on pressure recovery was encountered at the higher Mach numbers and at the greater oscillation amplitudes.

The photograph of shock oscillation at $M_0 = 1.35$ (fig. 15(a)) was obtained near rich blow-out. At $M_0 = 1.50$ the photographs for both smooth and pulsing operation were obtained at the same fuel-air ratio. The cause of the transition from smooth operation to an oscillating normal shock is not known; however, the 1.5-percent drop in diffuser total-pressure recovery was not sufficient to noticeably affect engine performance. At $M_0 = 1.35$ and 1.5 the amplitude of the shock movement was very small and it was difficult to determine frequencies from instantaneous pressure records. Where measurements could be made, the frequency was of the order of 45 cycles per second.

At $M_0 = 1.73$ (fig. 15(c)) the maximum normal shock movement encountered appears to be from a position just ahead of the inlet lip to near the midpoint of the exposed portion of the spike, a distance of approximately 2 inches. At this condition, the frequency was 46 cycles per second, and because the exposure time for the picture was greater than the time required for a complete cycle, the travel of the normal shock is evident. The extension of the oblique shock through the normal shock indicates that the shock pattern changed through approximately one full cycle during the time of exposure.

[redacted]

The operational data corresponding to the shadowgraph pictures under burning operation shown in figure 15 are included in figure 10.

1376

Several frames from a high-speed motion picture of a single cycle typical of the shock pulsations resulting at $M_0 = 1.73$ (same conditions as fig. 15(c)) are shown in figure 16. The cycle was completed in 33 frames, but the sequence can be shown just as well by every fourth frame. Although the cycle frequency was regular (46 cycles per second) the high-speed motion pictures indicate that the amplitude varied somewhat from cycle to cycle.

This amplitude variation is further verified by a simultaneous record of the variation in the instantaneous static pressure at the diffuser outlet (fig. 17). The fundamental frequency of adjacent cycles is constant, but the amplitude varies considerably. The zero or mean pressure was displaced from the center line of the grid; in general, the variation in pressure was symmetrical about the mean. The maximum variation in pressure for the trace shown is ±7.8 percent of the mean pressure. Excellent agreement was obtained between the frequencies determined from the high-speed motion pictures and those determined from the instantaneous pressure trace.

The combined subsonic and supersonic diffuser total-pressure recoveries for cold flow and for burning conditions are presented in figure 18. The cold-flow recoveries at $M_0 = 1.35$ and 1.73 are summarized in figure 18(a). The normal shock was at its design position, the lip of the diffuser, for $M_3 = 0.24$ at $M_0 = 1.35$ and $M_3 = 0.185$ at $M_0 = 1.73$. Apparently at $M_0 = 1.35$, the slight increase in subsonic-diffuser losses in the range of combustion-chamber-inlet Mach numbers where the normal shock approached the lip was of sufficient magnitude to cause a small general decline in the over-all pressure recovery with increases in M_3. At $M_0 = 1.73$, however, the characteristic peak in pressure recovery was observed at the design M_3. The highest cold recovery at $M_0 = 1.35$ and $M_3 = 0.142$ was 98.4 percent, whereas at the design M_3 the recovery was 96 percent. At $M_0 = 1.73$ the peak recovery was 89.1 percent and occurred at the design M_3. No appreciable shock pulsations were observed for the cold data presented.

The curves drawn through the cold-flow pressure-recovery data are included in figure 18(b), in which the pressure recoveries obtained under burning conditions are presented. In general, close

agreement was obtained between the cold and hot flow conditions, the scatter in the hot data being approximately ±1 percent. As previously indicated in the discussion of figure 11, the recovery at design and under subcritical operating conditions was above normal shock but less than the theoretical recovery at all three free-stream Mach numbers.

Only subcritical operation could be obtained at $M_0 = 1.35$ under burning conditions. It is not clear from the data in figure 18(b) whether the design M_3 was approached at $M_0 = 1.5$. Shadowgraph pictures indicated, however, that at M_3 above approximately 0.195 the flow was supercritical.

When compared to the curve established under cold-flow conditions, only two points are definitely supercritical at $M_0 = 1.73$. This is confirmed by the variation in static pressures on the spike (fig. 19). The four curves in figure 19 are for these two supercritical points, for the critical condition, and for the condition of figure 15(c) where $f/a = 0.072$ (M_3=0.144). All four of these points are plotted in figure 18. The normal shock for the condition shown in figure 15(c) occurs at approximately the midpoint of the exposed portion of the spike. A sudden change in static pressure such as experienced across a normal shock also occurred at this point. For the two points indicated as supercritical (those having M_3 of 0.198 and 0.200), the sudden rise in static pressure occurred within the inlet, whereas at the critical condition (M_3=0.185) the static-pressure rise occurred at the lip. It therefore appears that the static pressure on the spike may be reliably employed as an indication of the normal shock position.

Performance at Off-Design Spike Location

The combined subsonic and supersonic diffuser pressure recovery at $M_0 = 1.5$ under cold-flow conditions is presented in figure 20 for the on-design spike position and two off-design spike positions. The off-design spike positions chosen are those that would be on-design at $M_0 = 1.73$ and 1.35. The absolute values of pressure recovery presented in figure 20 are 2 to 3 percent low because, due to limited air-dryer capacity, these data were obtained with some condensation in the free-jet nozzle (air temperature = 110°; dew-point = 34° F), and the total-pressure loss due to condensation in

the nozzle is included in the values for diffuser pressure recovery. Inasmuch as the air temperature and dew point remained constant, however, the total-pressure loss across a condensation shock occurring in the nozzle would be constant, and the trends indicated in figure 20 may be considered valid.

Three shadowgraph pictures are shown for each spike position and their location on the pressure-recovery curve are indicated. The photographs correspond to subcritical, peak recovery, and supercritical operation and indicate the resulting inlet-shock structure. At the proper spike position for the free-jet Mach number at which these data were taken (M_0=1.50), a characteristic pressure-recovery curve was obtained with a peak at the condition at which the normal shock entered the engine (M_3=0.207).

Values as great as the peak design recovery and over a much wider range of burner inlet Mach numbers (0.165 - 0.195) resulted for the M_0 = 1.73 spike tip projection.

With the spike retracted beyond its design position (spike located for M_0=1.35), essentially normal shock recovery was obtained over the entire range of M_3 investigated. On the basis of pressure recovery alone and excluding drag considerations, the diffuser of a ram jet required to fly over a range of flight Mach numbers should be designed for the maximum M_0. From a net-propulsive-force consideration, however, diffuser drag must also be evaluated before a final design is selected.

SUMMARY OF RESULTS

The results of a free-jet investigation for a 16-inch ram jet at Mach numbers of 1.35, 1.50, and 1.73 are summarized as follows:

1. Excellent agreement was obtained between the combined subsonic and supersonic diffuser total-pressure recoveries for cold flow and burning conditions. Over a range of combustion-chamber-inlet Mach numbers from 0.17 to 0.20, the subsonic diffuser total-pressure recovery was approximately 99 percent. At all three Mach numbers, the supersonic diffuser recovery was above normal shock recovery but below the theoretical recovery for a single oblique shock diffuser with no internal contraction.

2. When the diffuser was operated with a tip projection which caused the oblique shock to fall ahead of the diffuser lip, pressure recoveries as high as that resulting from operation at the design tip projection were obtained. The high recoveries extended over a wide range of combustion-chamber-inlet Mach numbers.

3. The shock pulsations encountered at the conditions of this investigation had no serious effect on diffuser total-pressure recovery or engine operation. The frequency was of the order of 46 cycles per second, always occurred in the subcritical region of flow, and was of small amplitude. Close agreement was obtained between the frequencies obtained from high-speed motion pictures of the shadowgraph and records of the instantaneous static pressure at the combustion-chamber inlet.

4. At free-stream Mach numbers of 1.35 and 1.50, the best engine performance was not obtained at the largest nozzle-outlet area investigated. For a Mach number of 1.73, best engine performance was obtained at the largest outlet-area ratio investigated (0.739) from the standpoints of both net thrust coefficient and thrust specific fuel consumption. Maximum values of thrust coefficient were 0.61, 0.64, and 0.67 for Mach numbers of 1.35, 1.50, and 1.73, respectively. The corresponding values of thrust specific fuel consumption were 4.1, 4.3, and 3.7 pounds of fuel per hour per pound of thrust.

5. Burner performance and consequently engine performance were influenced by the radial position of the fuel injector. The lean blow-out limits could often be extended by changing the radial position of the fuel injector. The optimum fuel-injector radius varied with flame-holder design.

6. Better performance was obtained with a rake flame holder (fig. 7) than with a serrated annular baffle flame holder (fig. 8). The operable range of fuel-air ratio was narrow with the serrated annular baffle and operation at the largest outlet-area ratio was not possible at Mach numbers of 1.5 and 1.73.

7. At low combustion-chamber-inlet static pressures, some improvement in engine performance was obtained by using a 50-percent blend by volume of propylene oxide and gasoline instead of gasoline alone. At other conditions, however, there was little advantage in using the blend. Although combustion efficiencies were higher

with the blend, the heating value was so much lower that the thrust specific fuel consumption was greater than with gasoline.

Lewis Flight Propulsion Laboratory,
National Advisory Committee for Aeronautics,
Cleveland, Ohio.

REFERENCES

1. Perchonok, Eugene, Wilcox Fred A., and Sterbentz, William H.: Preliminary Development and Performance Investigation of a 20-Inch Steady-Flow Ram Jet. NACA ACR E6D05, 1946.

2. Perchonok, Eugene, Sterbentz, William H., and Wilcox, Fred A.: Performance of a 20-Inch Steady-Flow Ram Jet at High Altitudes and Ram-Pressure Ratios. NACA RM E6L06, 1947.

3. Howard, Ephriam M., Wilcox, Fred A., and Dupree, David T.: Combustion-Chamber Performance with Four Fuels in a Bumblebee 18-Inch Ram Jet Incorporating Various Rake- or Gutter-Type Flame Holders. NACA RM E8I01a, 1948.

4. Nussdorfer, T. J., Sederstrom, D. C., and Perchonok, E.: Investigation of Combustion in 16-Inch Ram Jet under Simulated Conditions of High Altitude and Mach Number. NACA RM E50D04, 1950.

5. Sterbentz, William H., and Wilcox, Fred A.: Investigation of Effects of Movable Exhaust-Nozzle Plug on Operational Performance of 20-Inch Ram Jet. NACA RM E8D22, 1949.

6. Connors, James F., and Schroeder, Albert H.: Experimental Investigation of Pressure Fluctuations in 3.6-Inch Ram Jet at Mach Number 1.92. NACA RM E9H12, 1949.

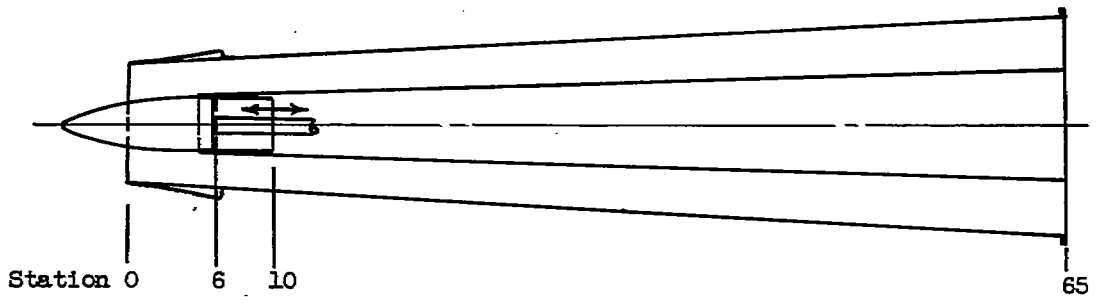

1376

TABLE I - COORDINATES OF 16-INCH RAM JET

Diffuser outer-body coordinates		Diffuser inner-body coordinates		Spike coordinates	
Station	Inside diameter (in.)	Station	Outside diameter (in.)	Distance from apex (in.)	Outside diameter (in.)
0	9.00	$4\frac{3}{4}$	4.00	0 to 3	46° cone
0 to 1	16° cone	$5\frac{3}{4}$	4.16	$3\frac{1}{2}$	2.94
1	9.28	6	4.19	$3\frac{3}{4}$	3.16
$1\frac{1}{2}$	9.36	$6\frac{1}{4}$	4.22	4	3.34
2	9.44	$6\frac{1}{2}$	4.25	$4\frac{1}{4}$	3.50
$2\frac{1}{2}$	9.52	$6\frac{3}{4}$	4.28	$4\frac{1}{2}$	3.64
3	9.60	$9\frac{3}{4}$	4.56	$4\frac{3}{4}$	3.72
$3\frac{1}{2}$	9.66	10	4.56	5	3.82
4	9.72	65	8.00	$5\frac{1}{4}$	3.88
$4\frac{1}{2}$	9.76	75	8.00	$5\frac{1}{2}$	3.92
5	9.82	91	6.00	$5\frac{3}{4}$	3.94
6	9.92			$6\frac{1}{4}$	3.98
65 to 172	16.00			$6\frac{1}{2}$ to $9\frac{3}{4}$	4.00
181	13.75				

[redacted]

TABLE II - SUMMARY OF PERFORMANCE OF 16-INCH RAM JET WITH RAKE FLAME HOLDER

Mach number M_0	Altitude (ft)	Air temperature (°F ±10°)	Outlet area ratio A_6/A_4	Fuel-air ratio range f/a		Peak combustion efficiency η_b		Mach number M_3 range		Peak total-temperature ratio, τ		Minimum specific fuel consumption W_f/F_n		Peak net thrust coefficient C_F		Peak pressure recovery P_3/P_0	
				Lean	Rich	η_b	f/a	Lean	Rich	τ	f/a	W_f/F_n	f/a	C_F	f/a	P_3/P_0	M_3
1.35	30,000	100	0.739	0.041	0.077	69.9	0.048	0.198	0.166	5.34	0.073	3.86	0.045	0.609	0.073	0.976	0.179
			.676	.043	.075	78.1	.043	.177	.156	5.51	.063	3.37	.043	.603	.070	.976	.162
			.650	.041	.074	77.7	.052	.174	.148	5.71	.072	3.32	.041	.603	.072	.976	.167
			.600	.044	.076	78.4	.057	.159	.137	5.88	.070	3.38	.044	.580	.070	.979	.140
1.50	35,000	110	.739	.053	.079	68.8	.053	.183	.169	5.31	.074	3.68	.053	.646	.079	.935	.183
			.676	.049	.081	76.7	.056	.173	.149	5.94	.081	3.40	.056	.648	.081	.931	.175
			.600	.046	.076	74.9	.049	.159	.140	5.75	.069	3.23	.046	.593	.069	.928	.152
			.550	.034	.066	71.0	.059	.200	.133	5.46	.066	3.62	.059	.620	.066	.921	.169
			.512	.033	.059	62.0	.059	.197	.137	4.68	.059	3.99	.059	.460	.059	.929	.197
1.75	41,000	160	.739	.048	.069	66.8	.059	.200	.185	4.58	.065	3.43	.048	.669	.065	.884	.185
			.676	.044	.067	64.0	.049	.197	.173	4.60	.067	3.35	.044	.639	.067	.879	.179
			.600	.048	.071	67.2	.050	.179	.159	4.38	.071	3.20	.050	.584	.071	.885	.159
			.550	.042	.072	61.0	.065	.177	.144	4.67	.072	3.53	.050	.567	.072	.890	.072

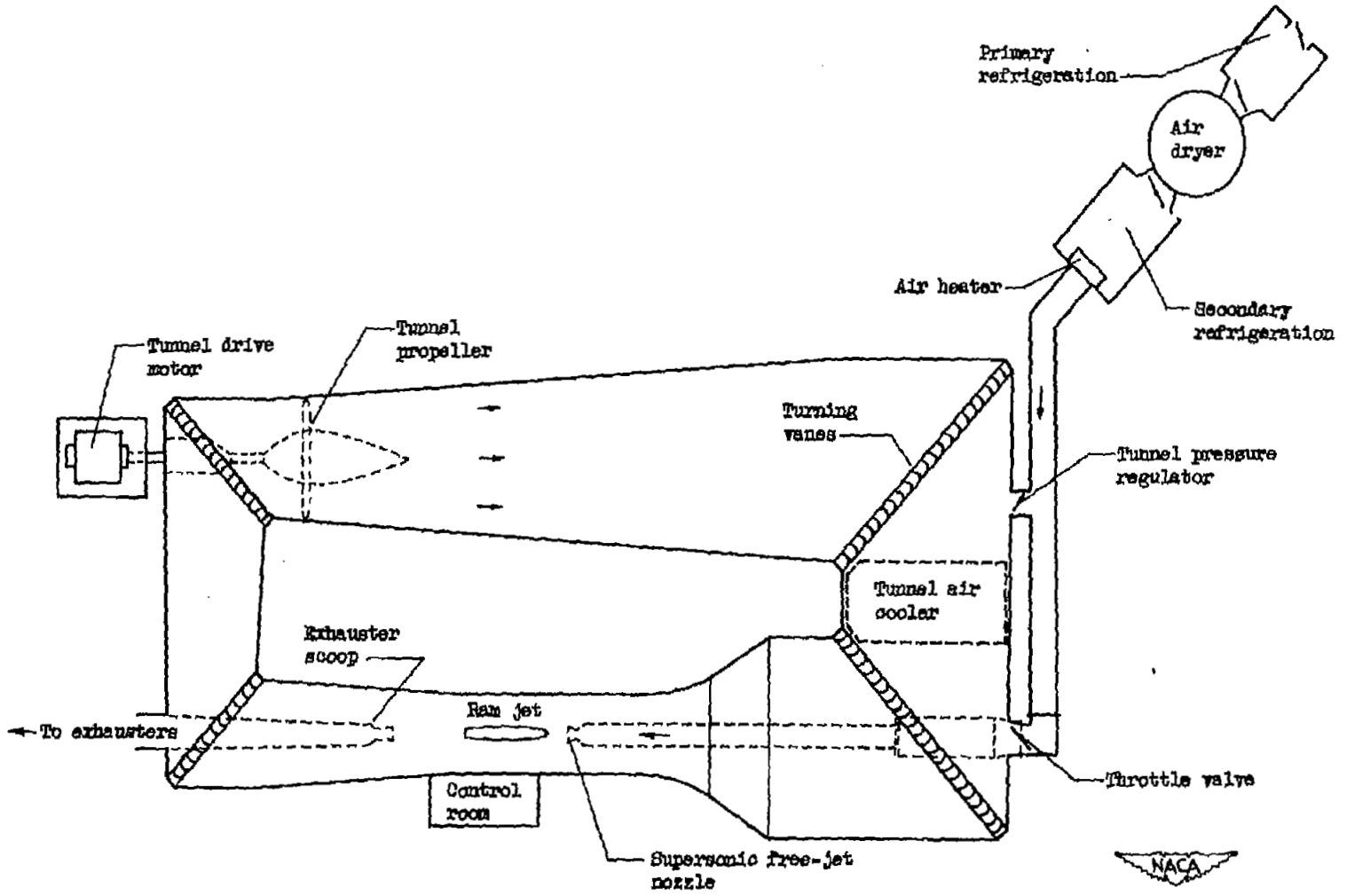

Figure 1. - Altitude-wind-tunnel free-jet facility.

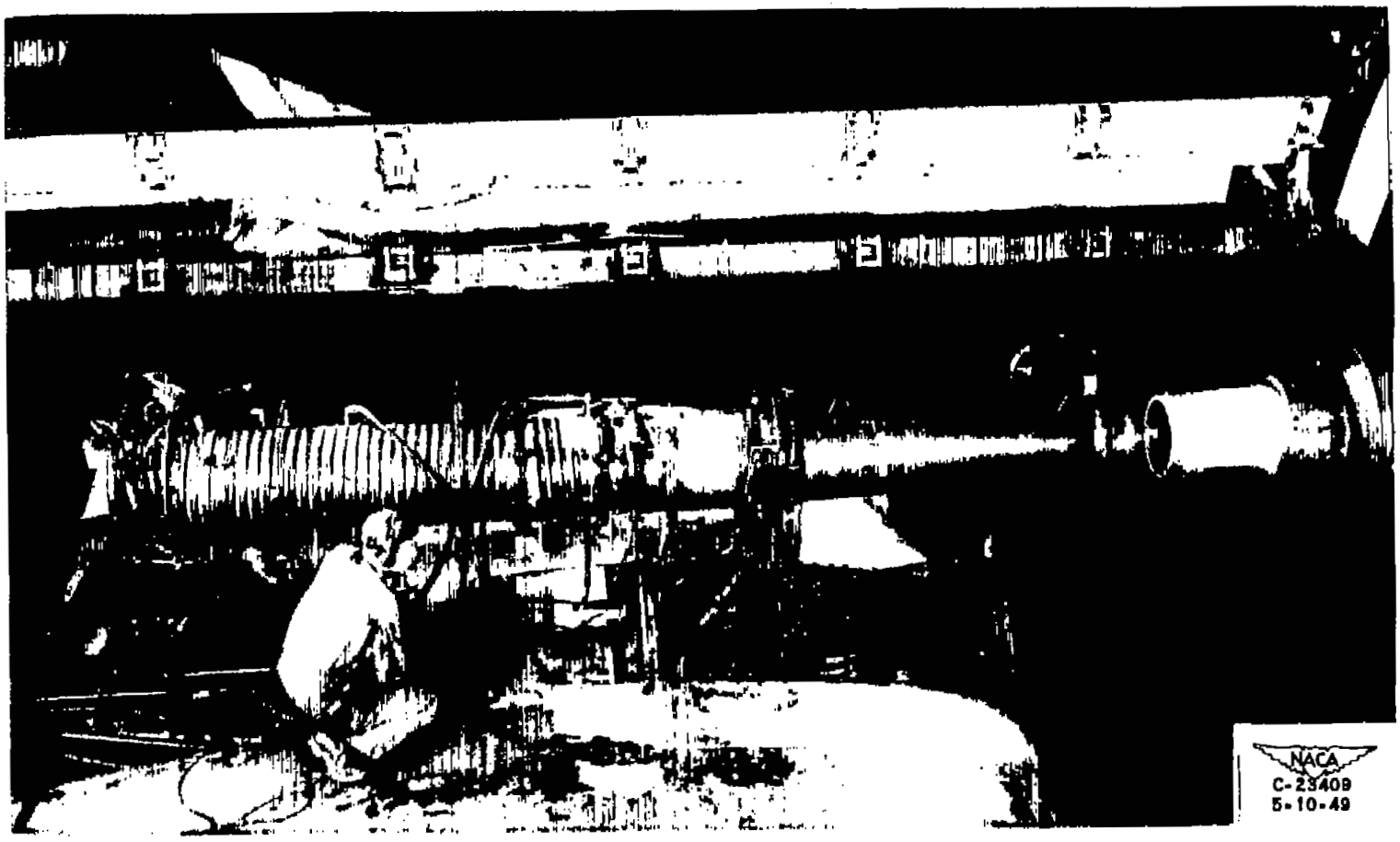

Figure 2. - Free-jet installation of 16-inch ram jet in altitude wind tunnel.

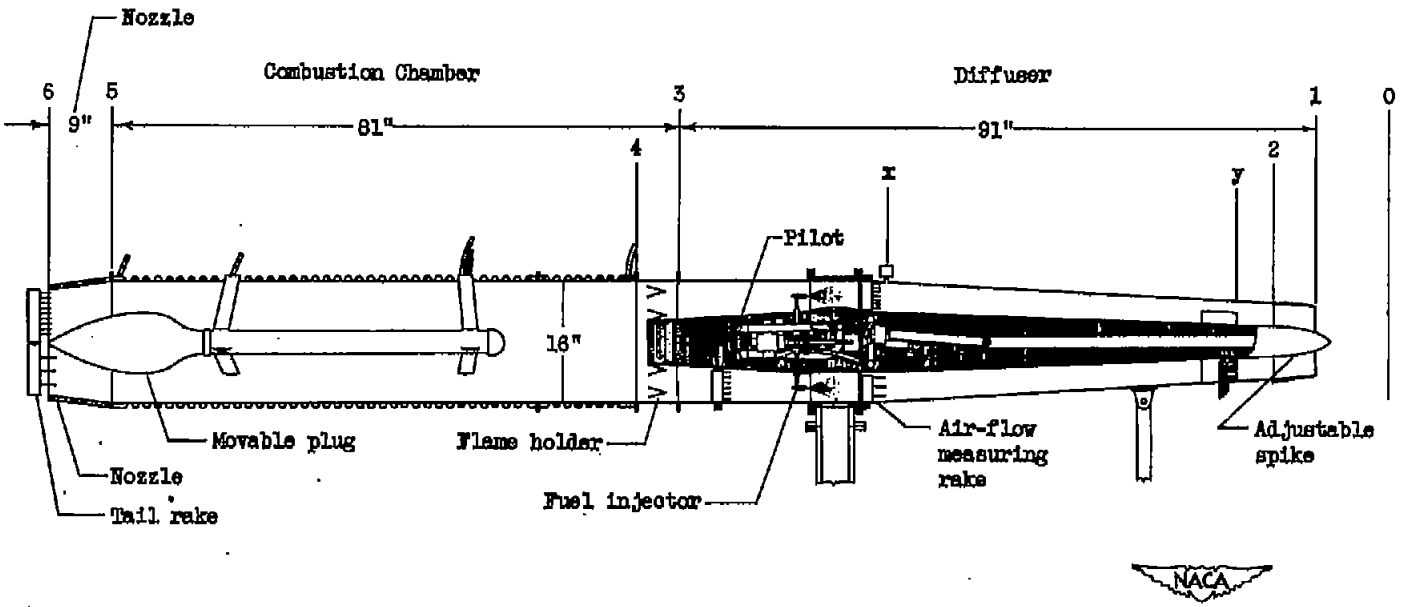

Figure 3. - Schematic diagram of 16-inch ram jet.

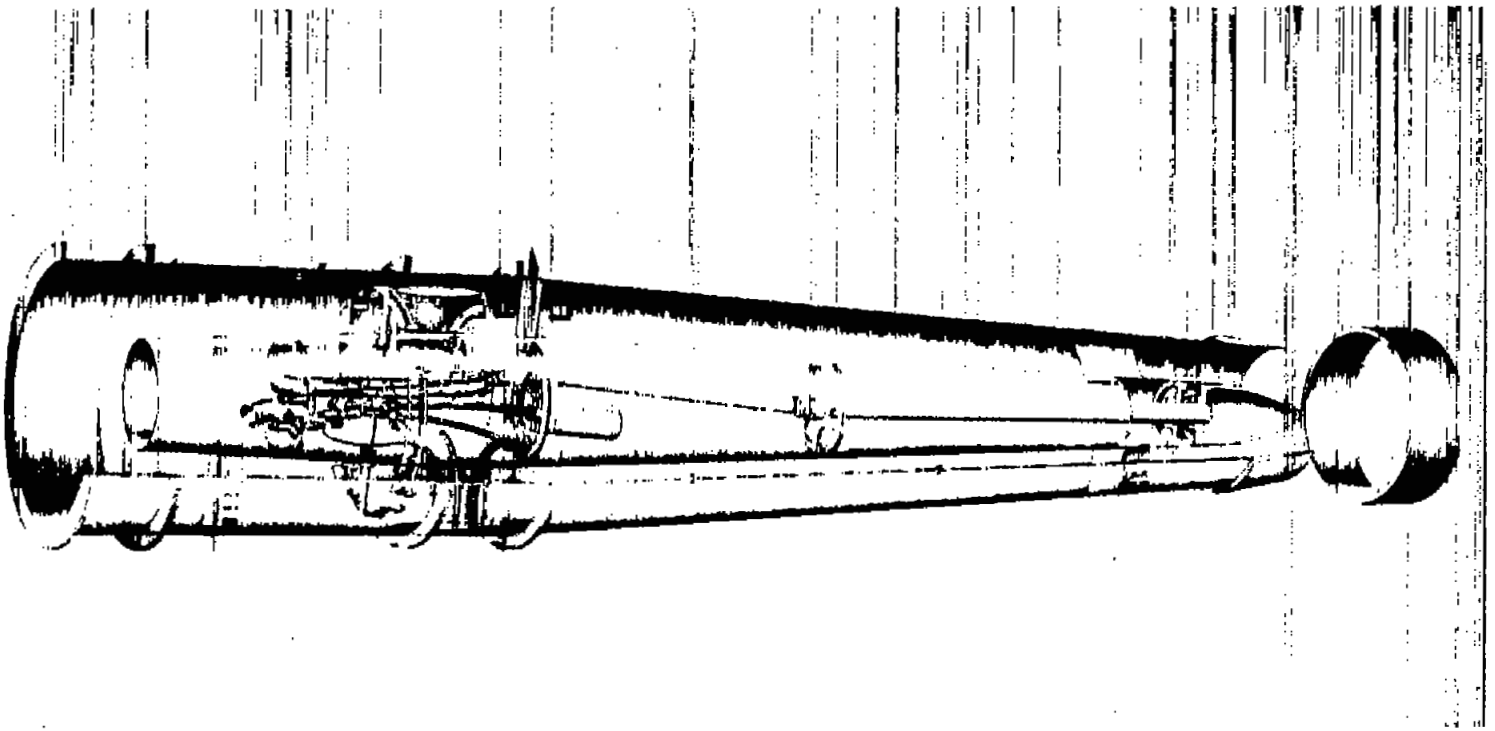

Figure 4. - Sketch of fuel bar actuating mechanism and pilot burner of 16-inch ram jet.

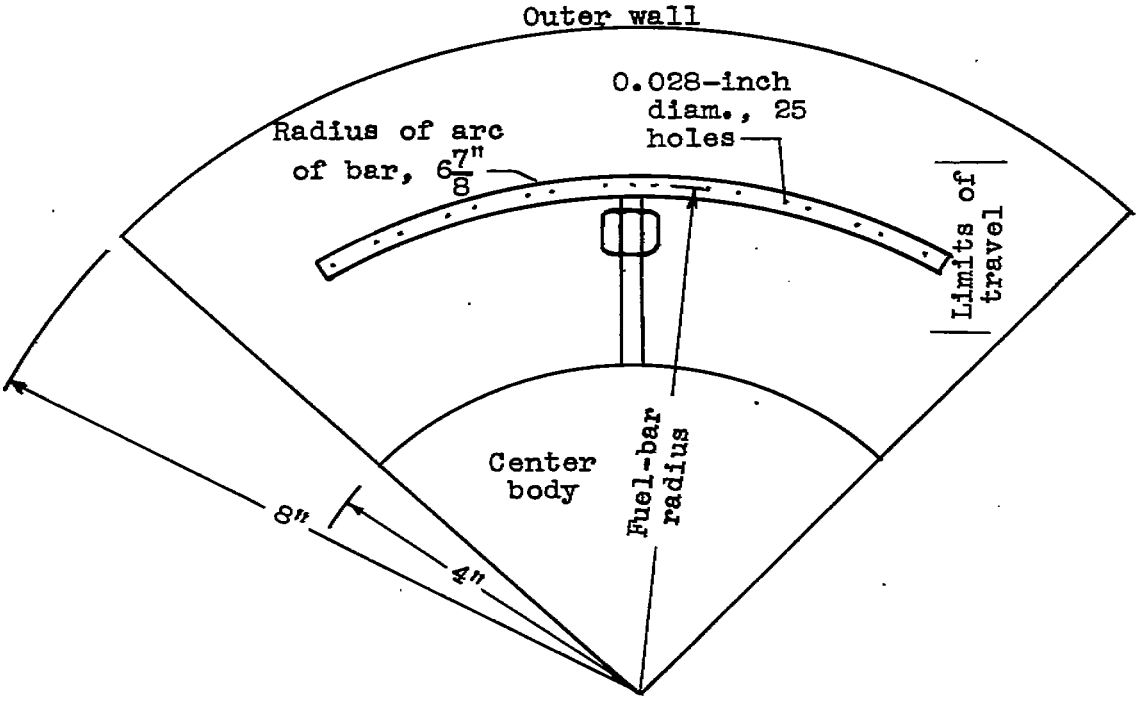

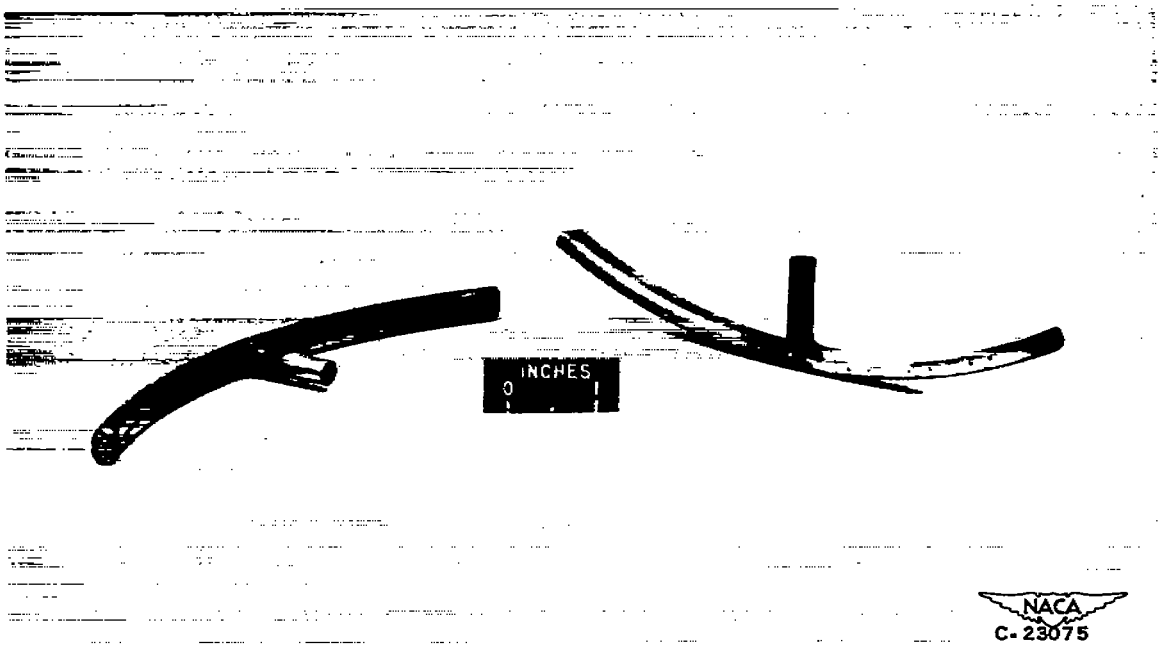

Figure 5. - Orifice fuel injector.

[redacted]

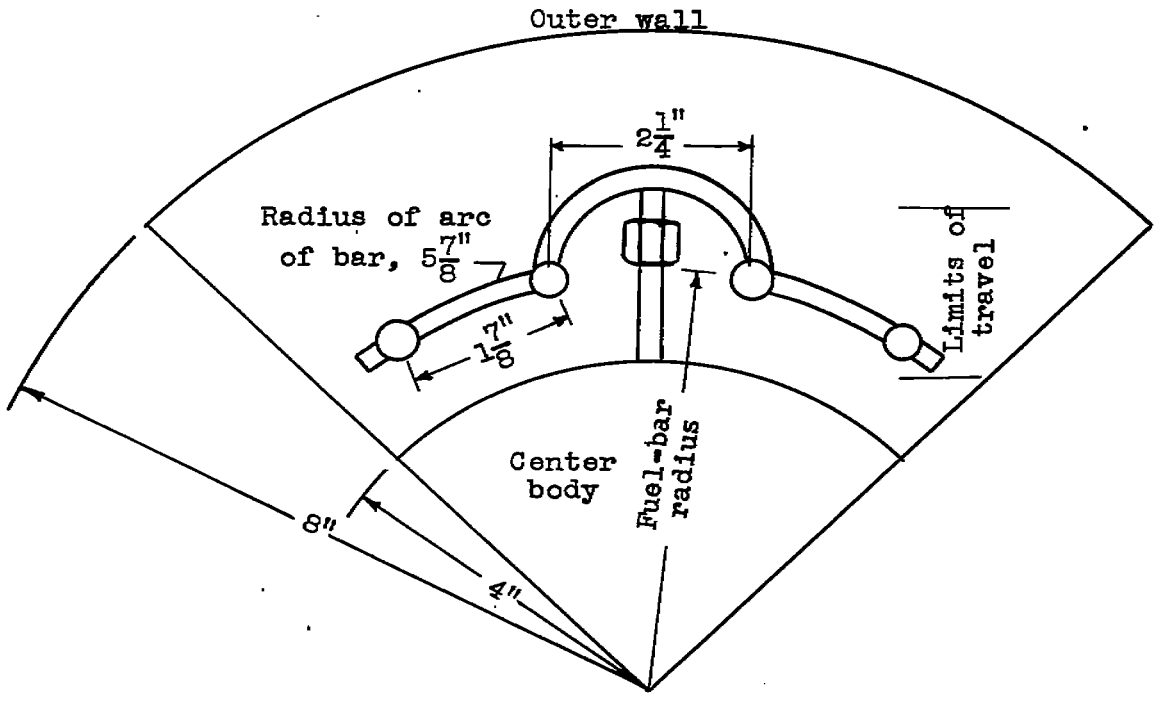

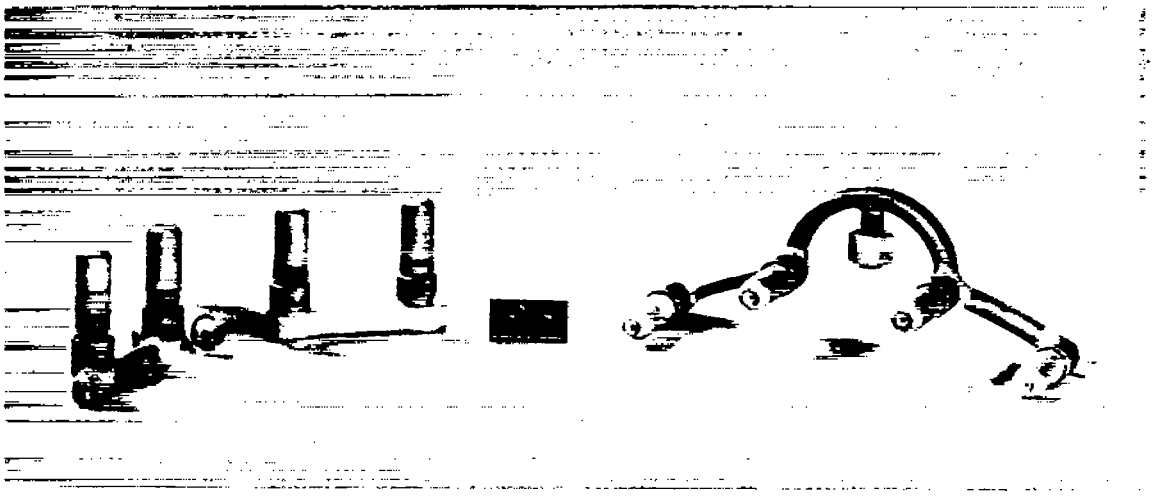

NACA
C-24142

Figure 6. - Spray-nozzle fuel injector.

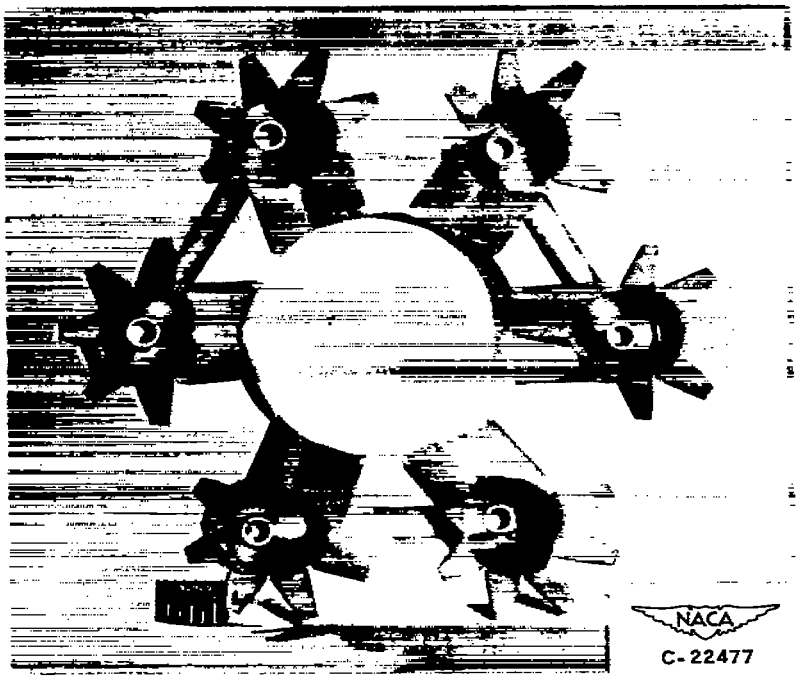

(a) Downstream view.

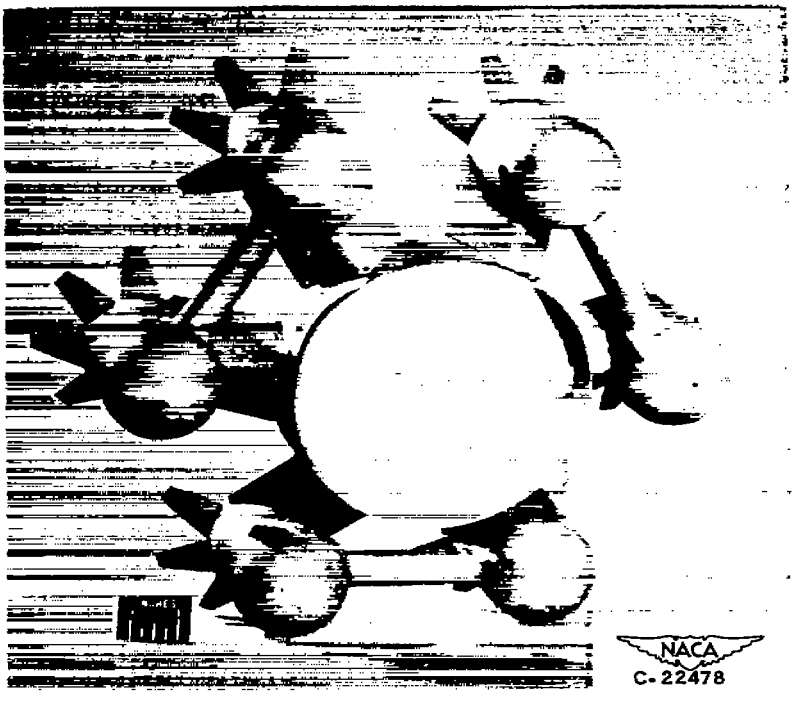

(b) Upstream view.

Figure 7. - Rake flame holder.

[redacted]

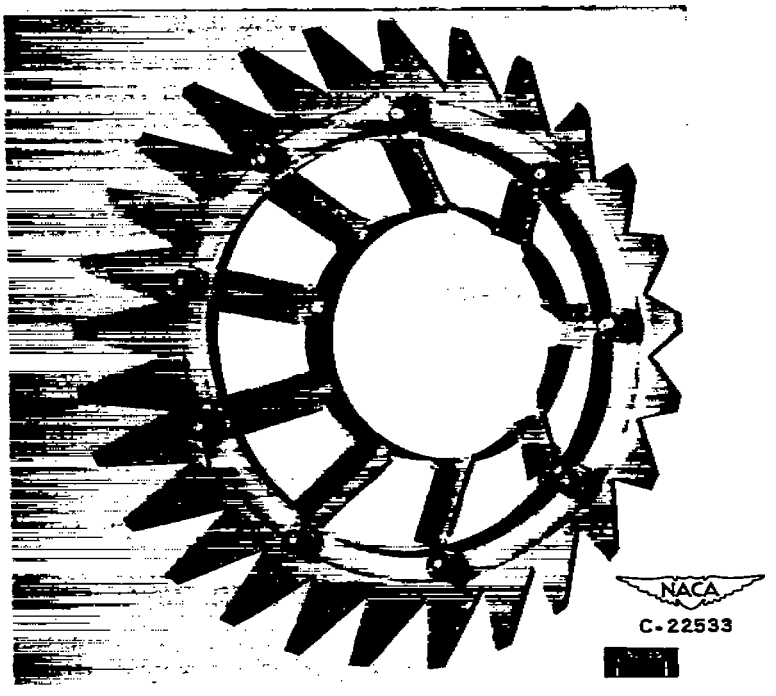

(a) Downstream view.

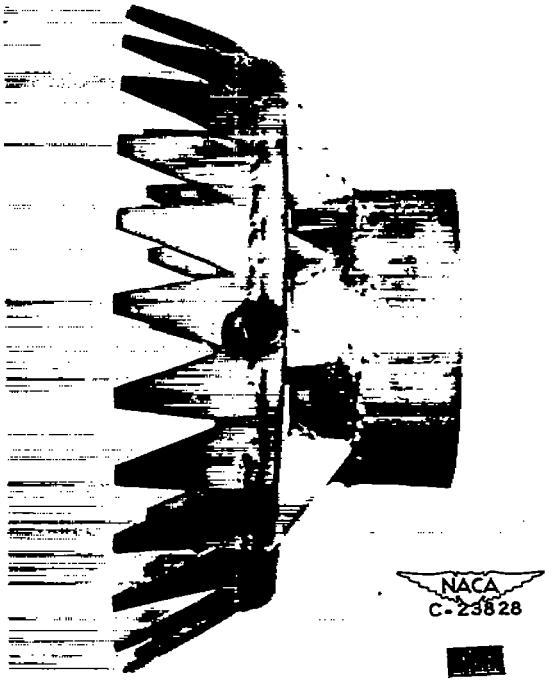

(b) Side view.

Figure 8. - Serrated annular baffle flame holder.

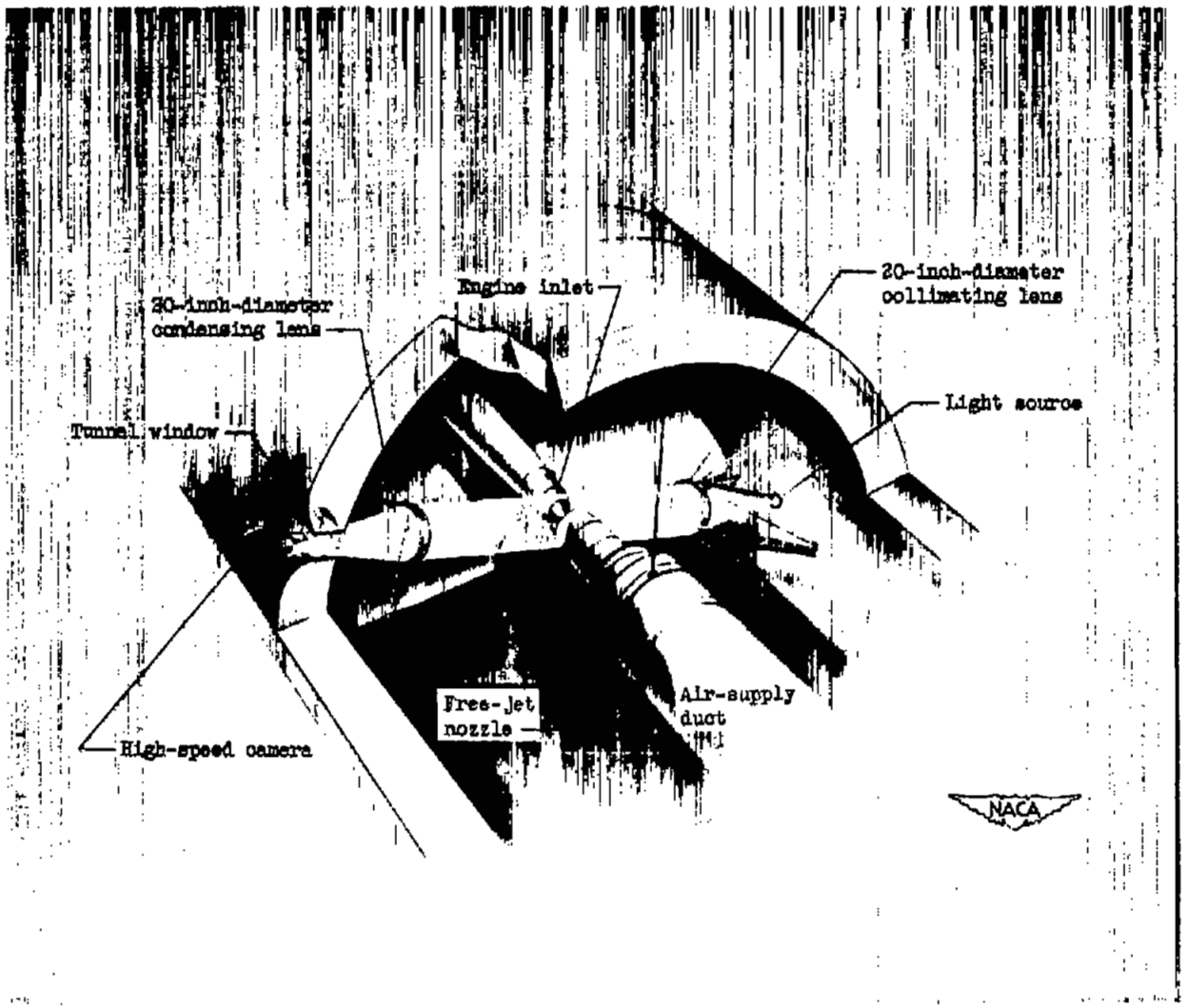

Figure 9. - Sketch of shadowgraph installation.

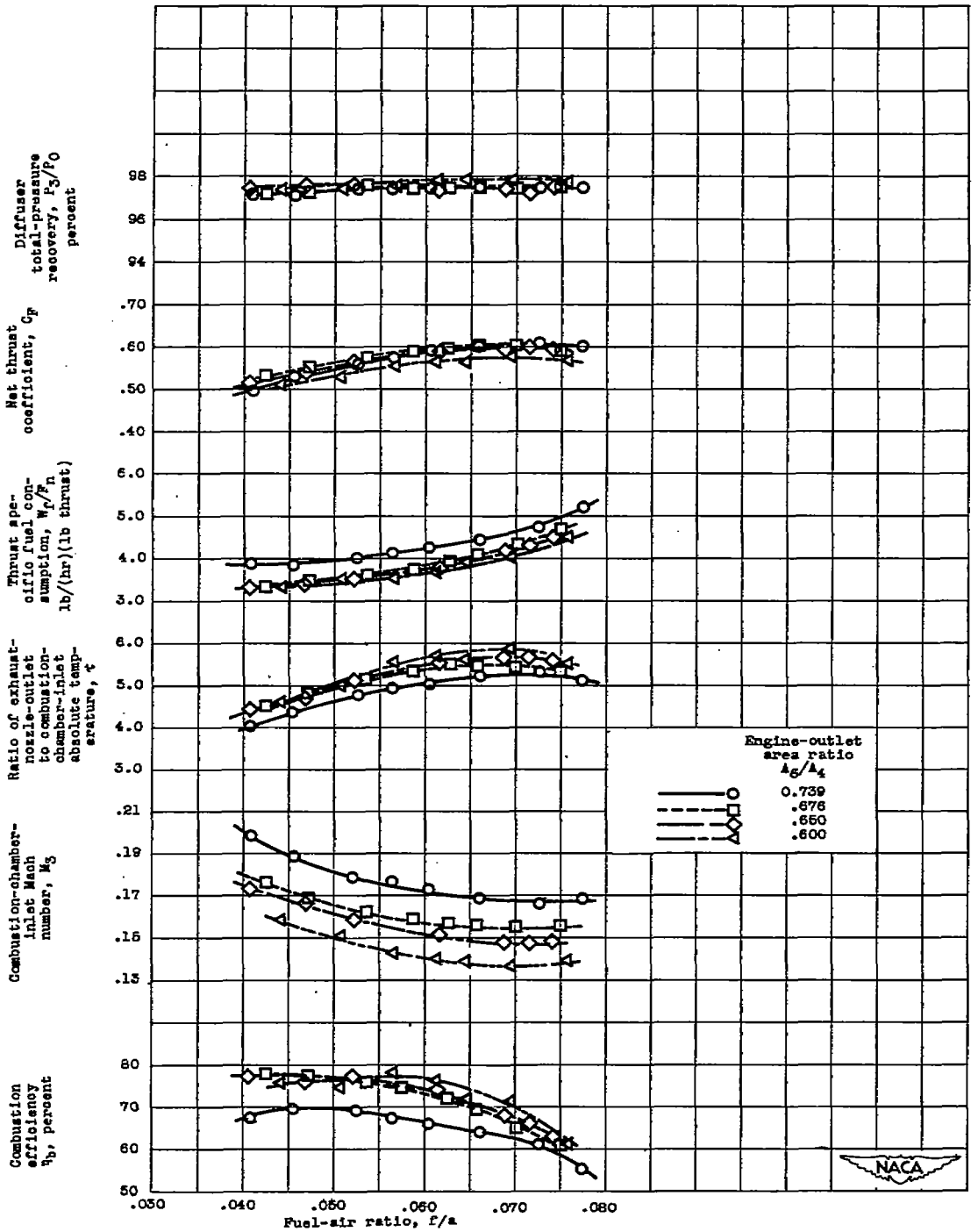

(a) Free-stream Mach number, M_0, 1.35; combustion-chamber-inlet static pressure, P_3, 1760 to 1780 pounds per square foot absolute; combustion-chamber-inlet static temperature, t_3, 100° ±10° F; altitude, 30,000 feet.

Figure 10. - Performance of 16-inch ram-jet with rake flame holder and orifice fuel injector.

[redacted]

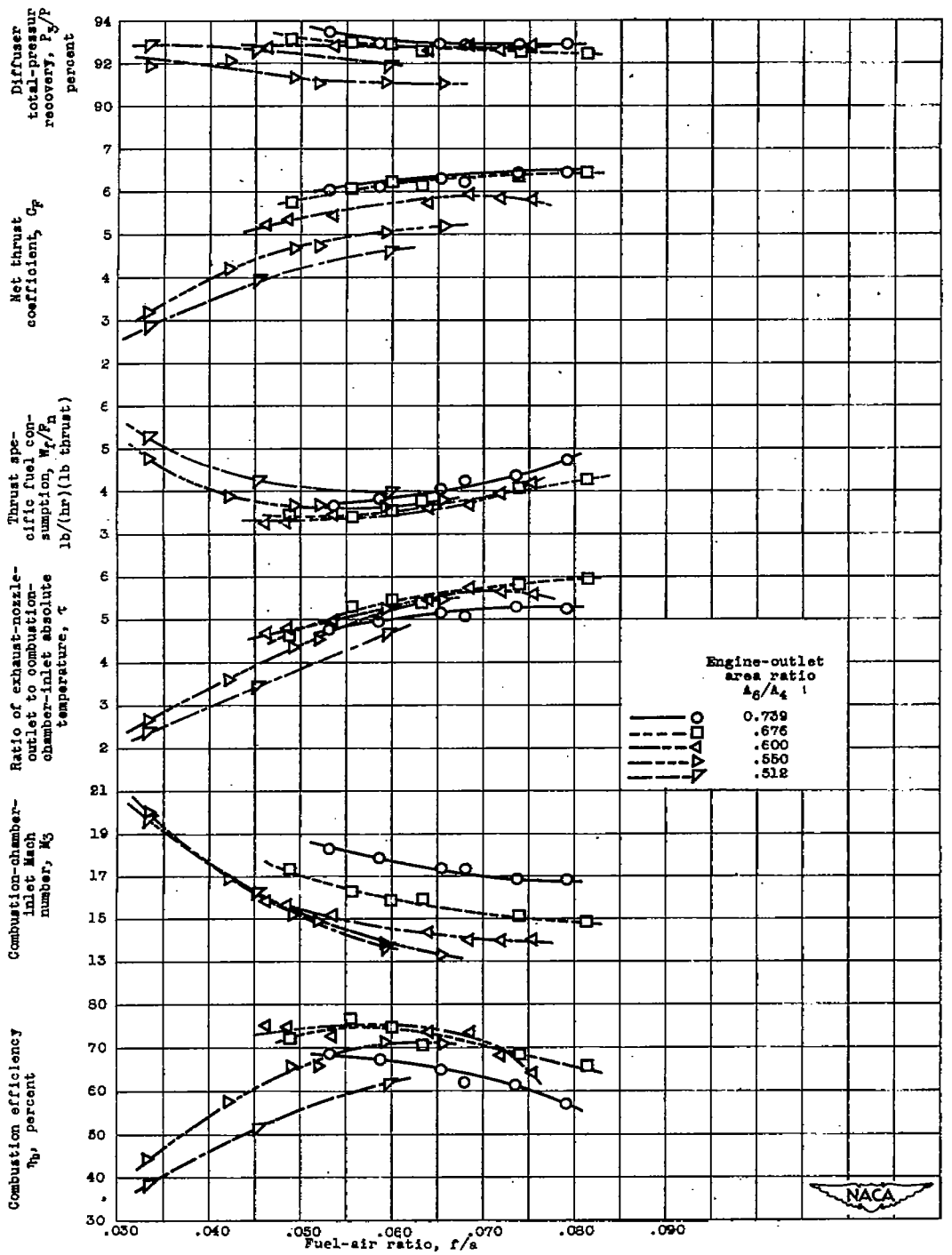

(b) Free-stream Mach number, M_0, 1.60; combustion-chamber-inlet static pressure, p_3, 1620 to 1670 pounds per square foot absolute; combustion-chamber-inlet static temperature, t_3, 110° ±10° F; altitude, 35,000 feet.

Figure 10. - Continued. Performance of 16-inch ram-jet with rake flame holder and orifice fuel injector

[redacted]

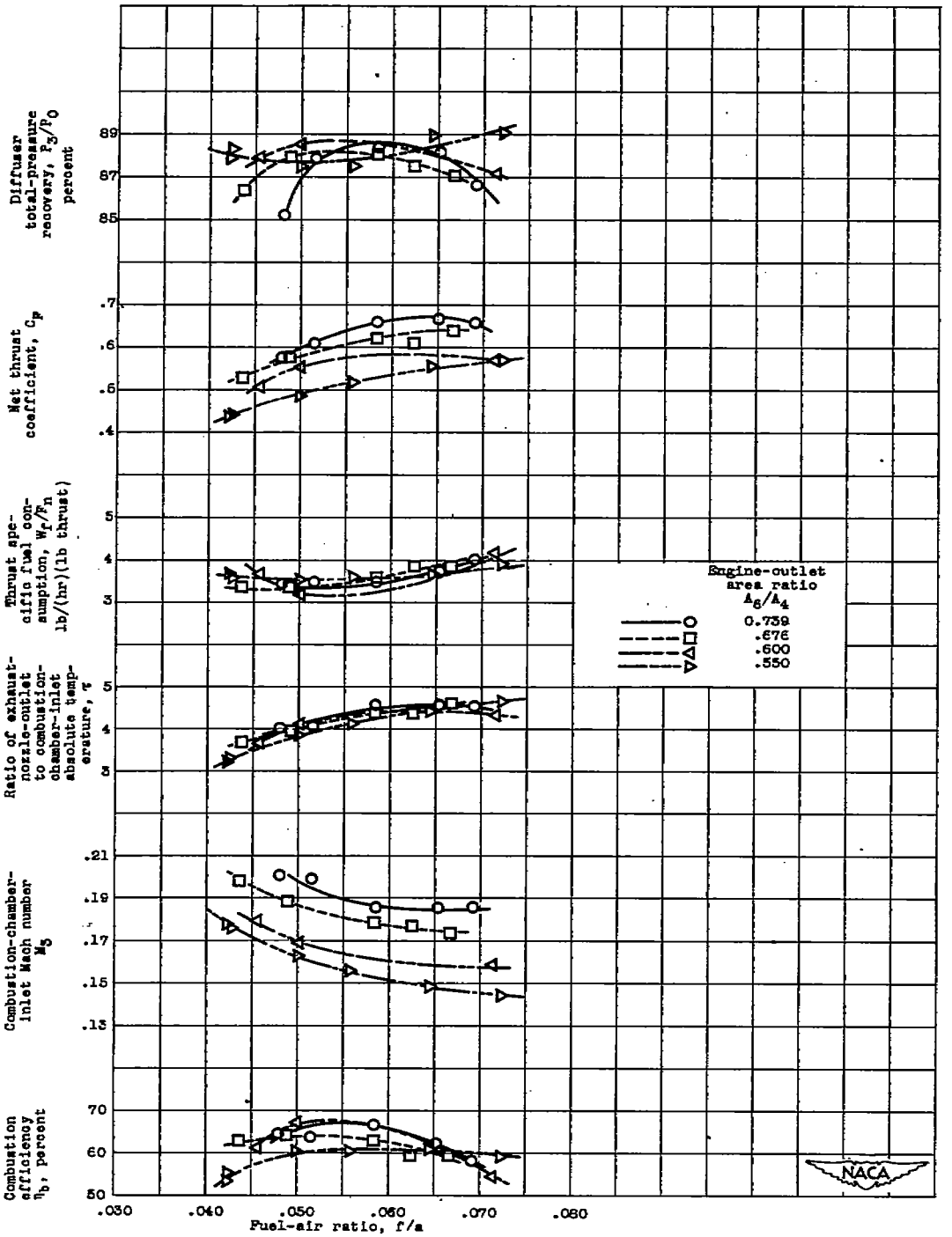

(c) Free-stream Mach number, M_0, 1.73; combustion-chamber-inlet static pressure, p_3, 1620 to 1670 pounds per square foot absolute; combustion-chamber-inlet static temperature, t_3, 160° ±10° F; altitude, 41,000 feet.

Figure 10. - Concluded. Performance of 16-inch ram-jet with rake flame holder and orifice fuel injector.

[redacted]

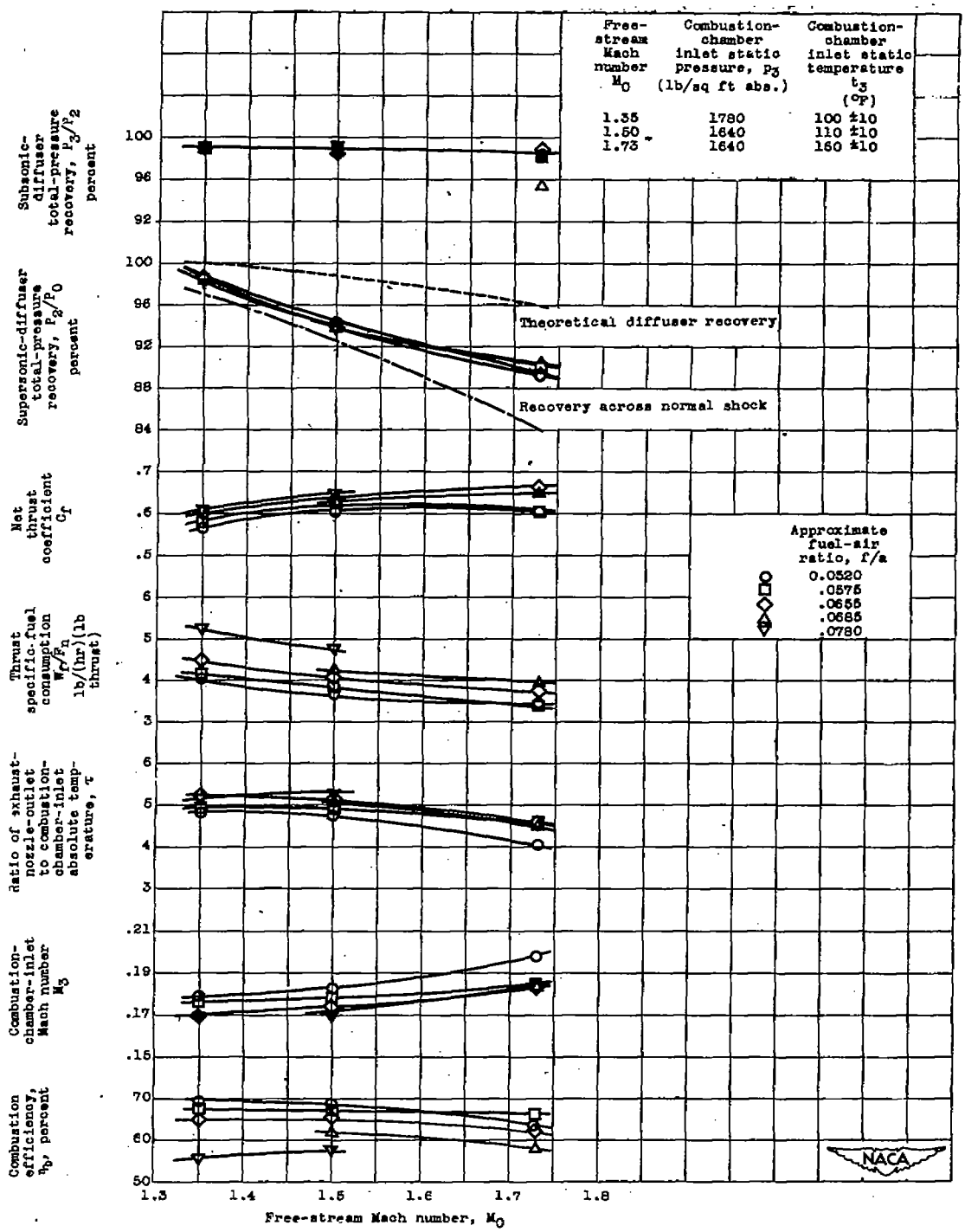

Figure 11. - Effect of free-stream Mach number on engine performance. Rake flame holder and orifice fuel injector. Engine-outlet area ratio, A_8/A_4, 0.739.

[redacted]

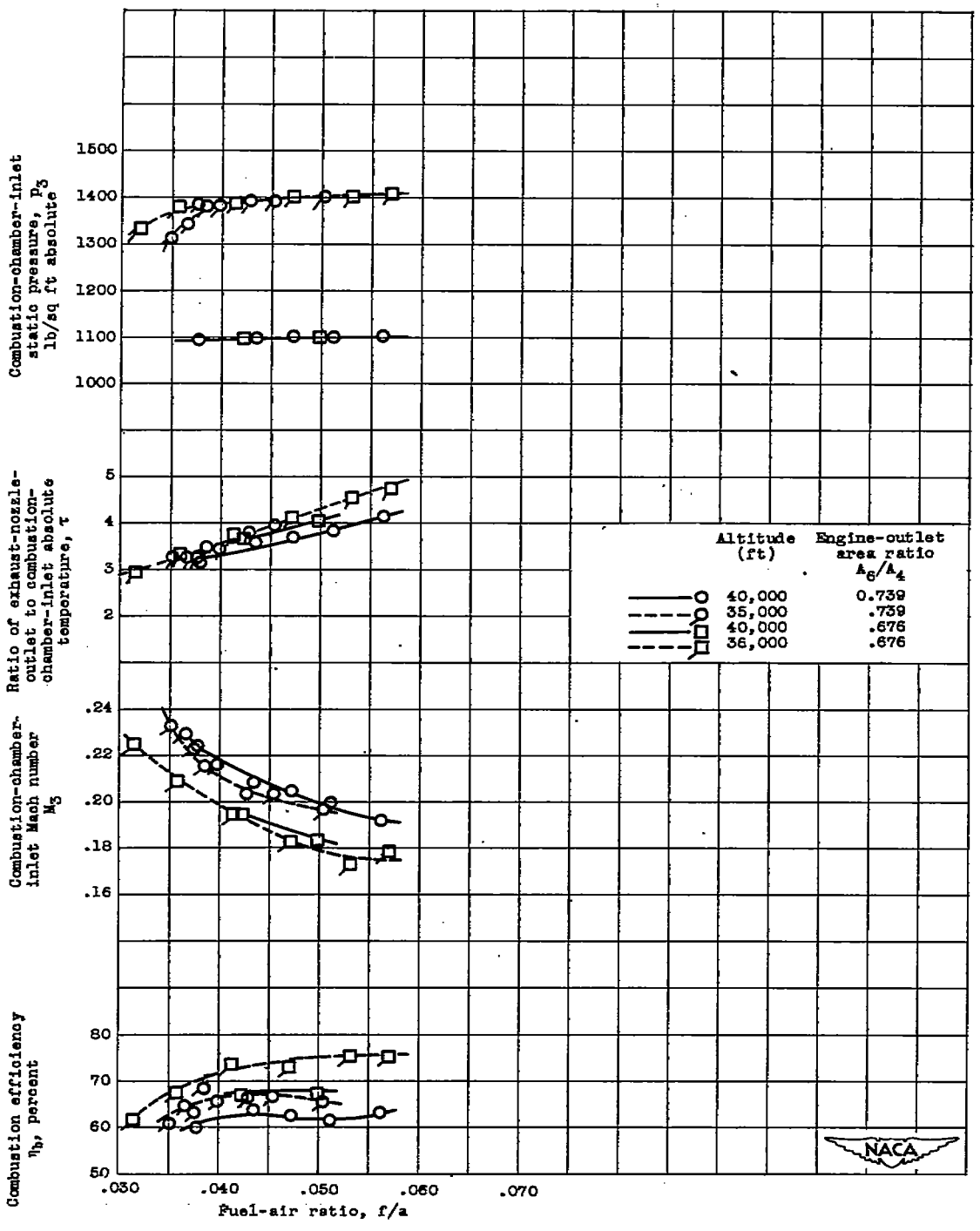

(a) Spray nozzle injector.

Figure 12. - Effect of fuel injector on 16-inch ram-jet combustion-chamber performance. Free-stream Mach number M_0, 1.35; fuel, 50 percent propylene oxide and 50 percent gasoline; combustion-chamber-inlet static temperature, 100° ±10° F.

[redacted]

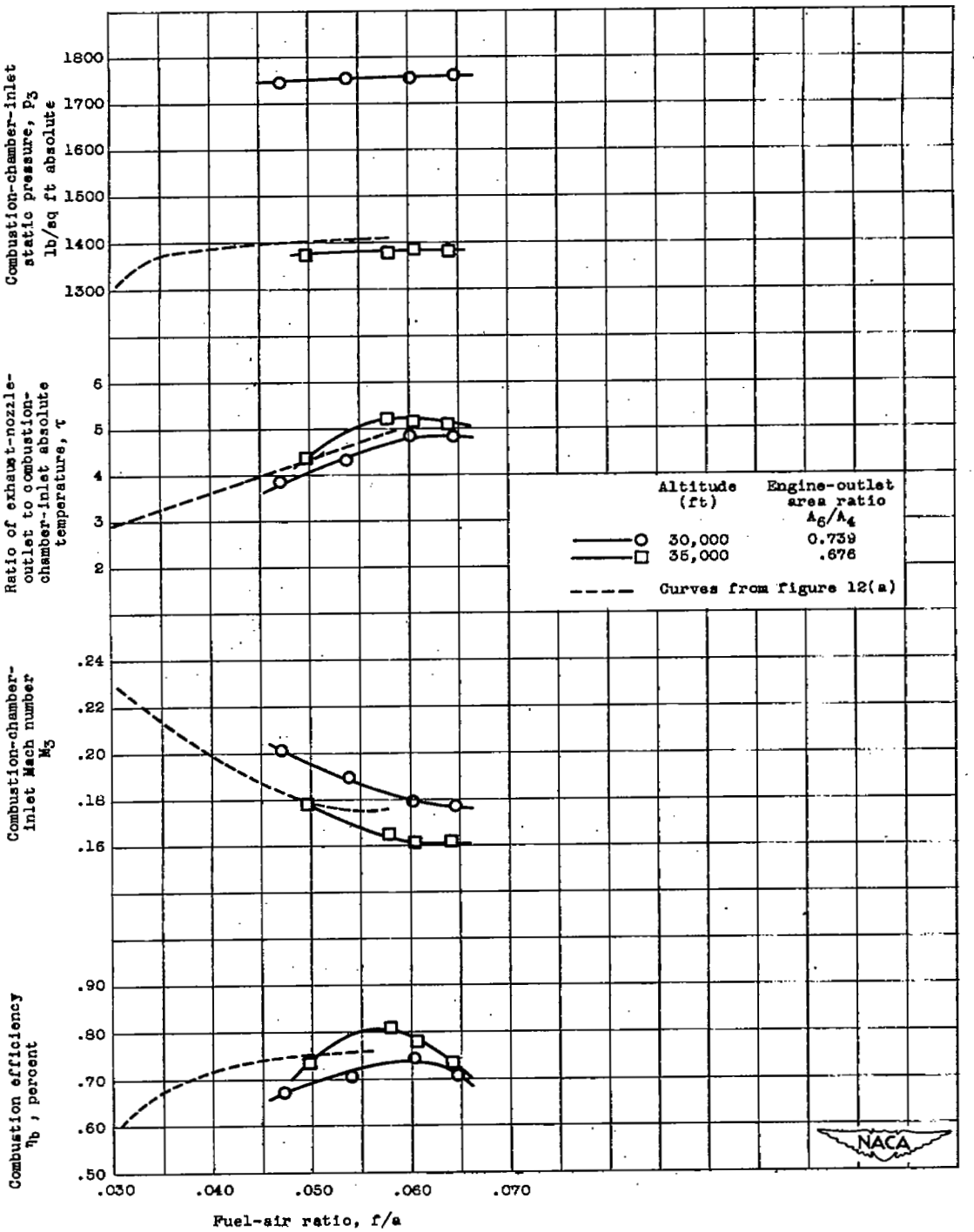

(b) Orifice injector.

Figure 12. - Concluded. Effect of fuel injector on 16-inch-ram-jet combustion-chamber performance. Free-stream Mach number M_0, 1.35; fuel, 50 percent propylene oxide and 50 percent gasoline; combustion-chamber-inlet static temperature, 100° ± 10° F.

[redacted]

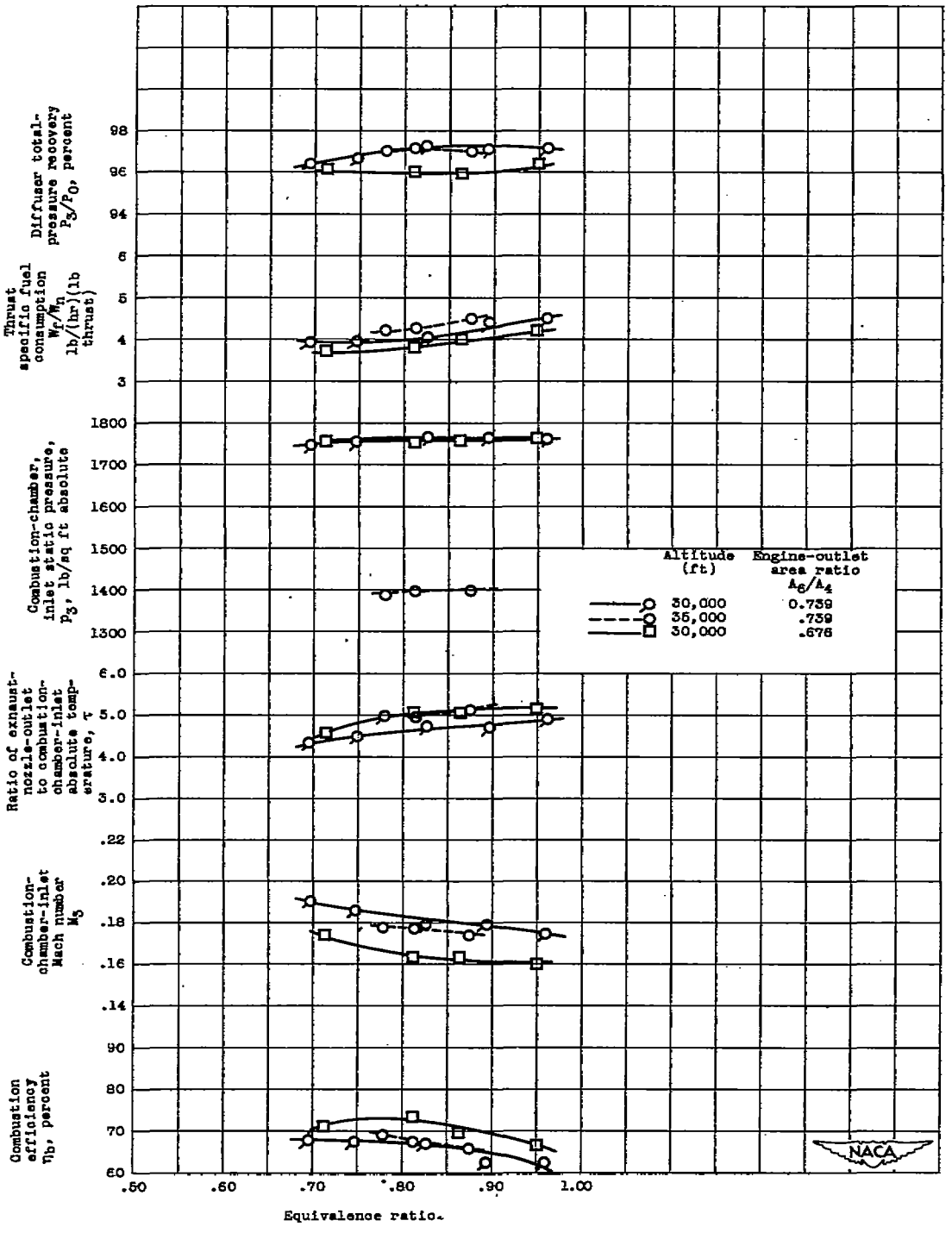

(a) Fuel, gasoline.

Figure 13. - Effect of fuel on 16-inch ram-jet combustion-chamber performance. Free-stream Mach number, M_0, 1.35; orifice fuel injector; combustion-chamber-inlet static temperature t_3, 100° ± 10° F.

[redacted]

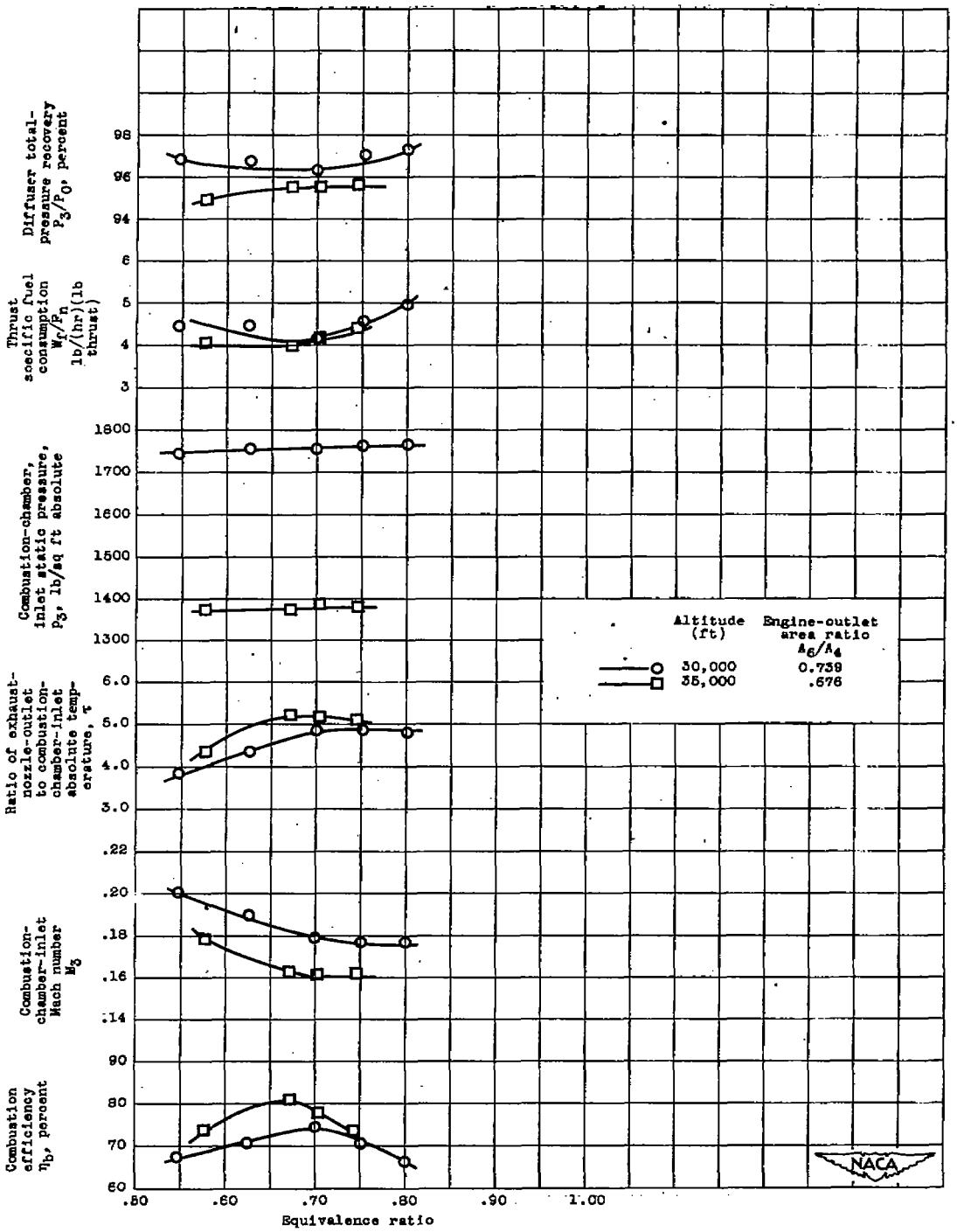

(b) Fuel, 50-percent mixture by volume of gasoline and propylene oxide.

Figure 13. - Concluded. Effect of fuel on 16-inch ram-jet combustion-chamber performance. Free-stream Mach number, M_0, 1.35; orifice fuel injector; combustion-chamber-inlet static temperature t_3, 100° ± 10° F.

[redacted]

7

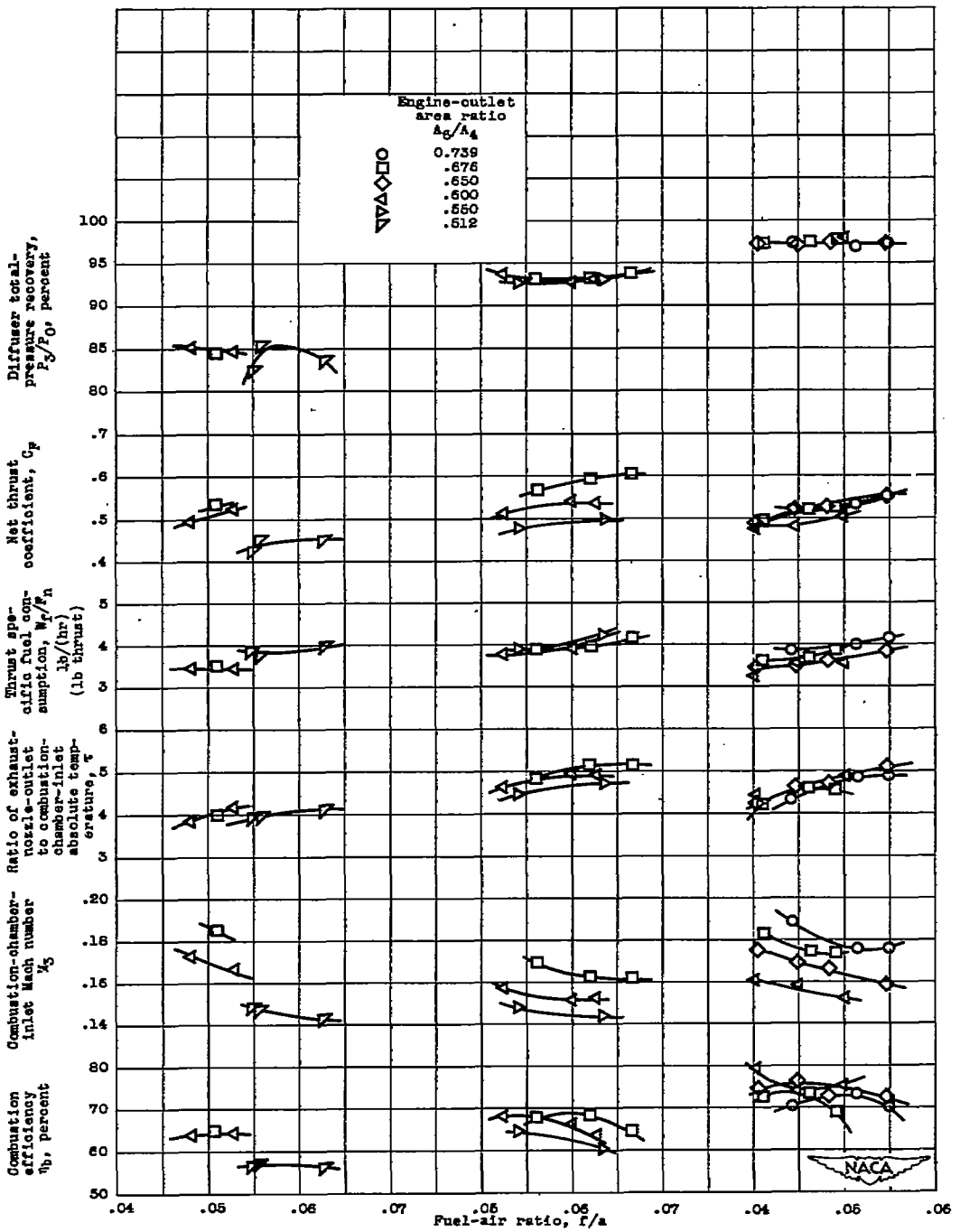

(a) M_0, 1.75; p_3, 1648 to 1752 pounds per square foot absolute; t_3, 160° ±15° F.

(b) M_0, 1.50; p_3, 1667 to 1681 pounds per square foot absolute; t_3, 110° ±15° F.

(c) M_0, 1.35; p_3, 1764 to 1786 pounds per square foot absolute; t_3, 110° ±10° F.

Figure 14. - Combustion-chamber performance of 16-inch ram jet with serrated annular baffle flame holder and orifice fuel injector.

[redacted]

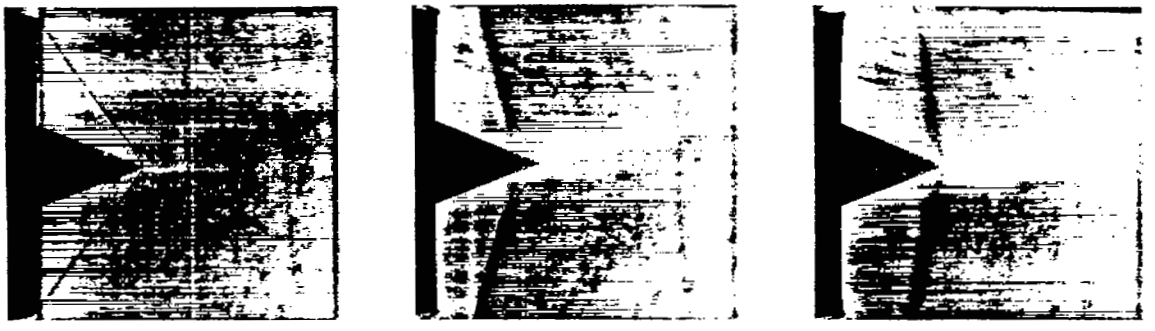

No burning | f/a = 0.041, P_3/P_0 = 0.972 | f/a = 0.077, P_3/P_0 = 0.975, Pulsing

(a) M_0 = 1.35; A_6/A_4 = 0.739.

No burning | f/a = 0.052, P_3/P_0 = 0.925 | f/a = 0.052, P_3/P_0 = 0.910, Pulsing

(b) M_0 = 1.5; A_6/A_4 = 0.550.

No burning | f/a = 0.072, P_3/P_0 = 0.890 | f/a = 0.050, P_3/P_0 = 0.874, Pulsing

(c) M_0 = 1.73; A_6/A_4 = 0.550.

NACA
C-26205
7-14-50

Figure 15. - Representative shadowgraph pictures at free-stream Mach numbers of 1.35, 1.5, and 1.73.

[redacted]

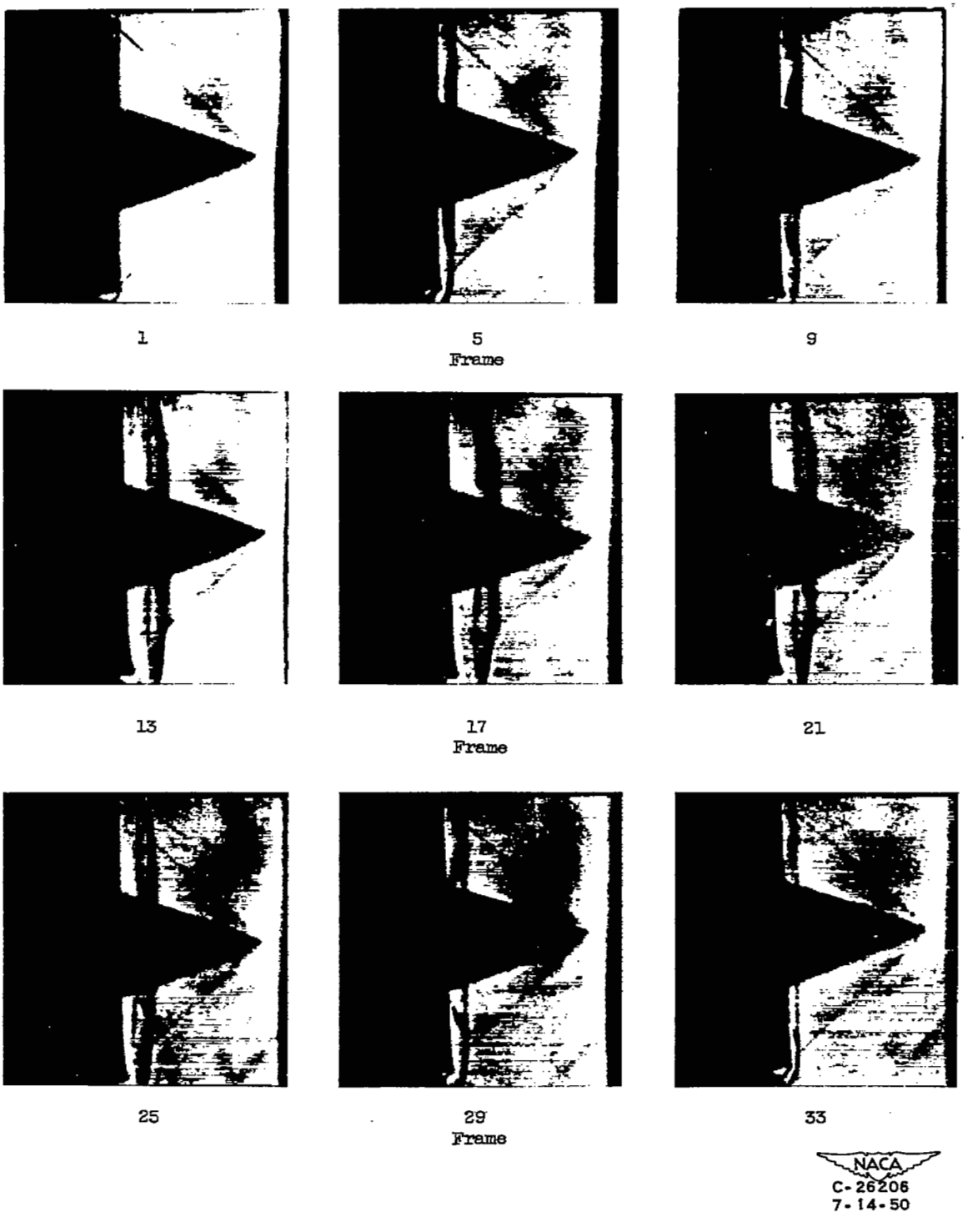

Figure 16. - Scenes from motion picture of pulsating shock at free-stream Mach number of 1.73. Frequency, 46 cycles per second.

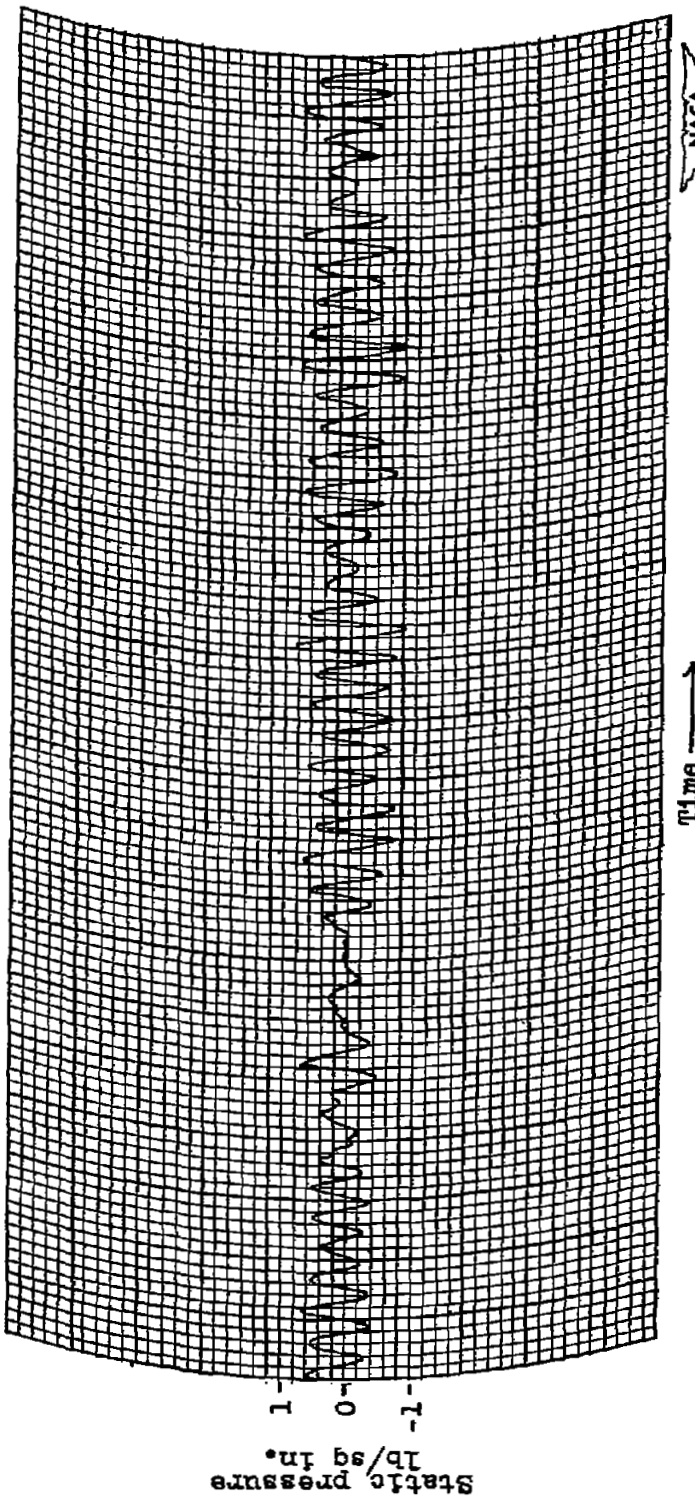

Figure 17. - Instantaneous static pressure variation at diffuser outlet. (Frequency, 46 cycles per second; amplitude, ± 7.8 percent of mean pressure.)

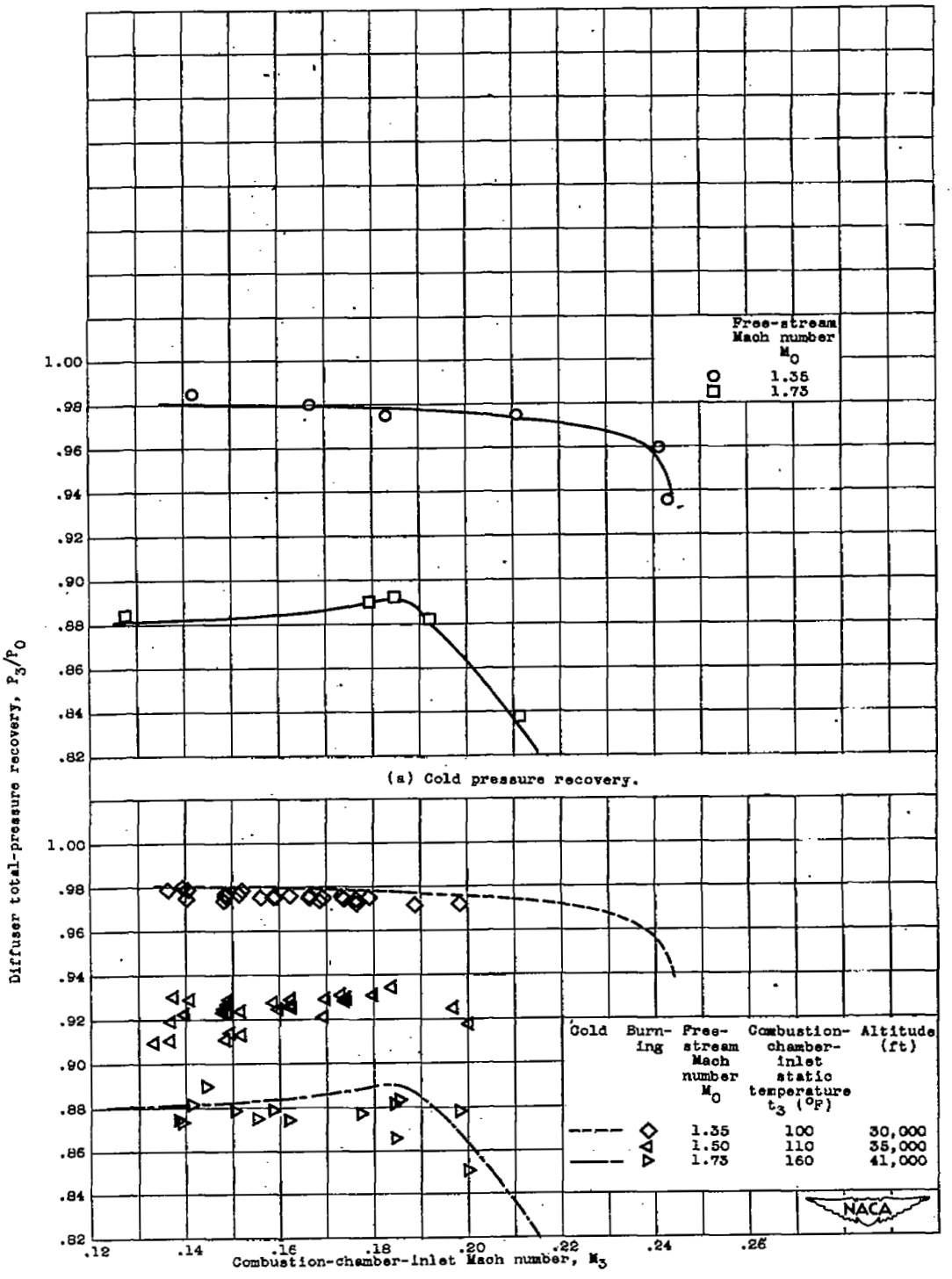

(b) Burning pressure recovery.

Figure 18. - Combined subsonic and supersonic diffuser total-pressure recoveries for 16-inch ram jet.

[redacted]

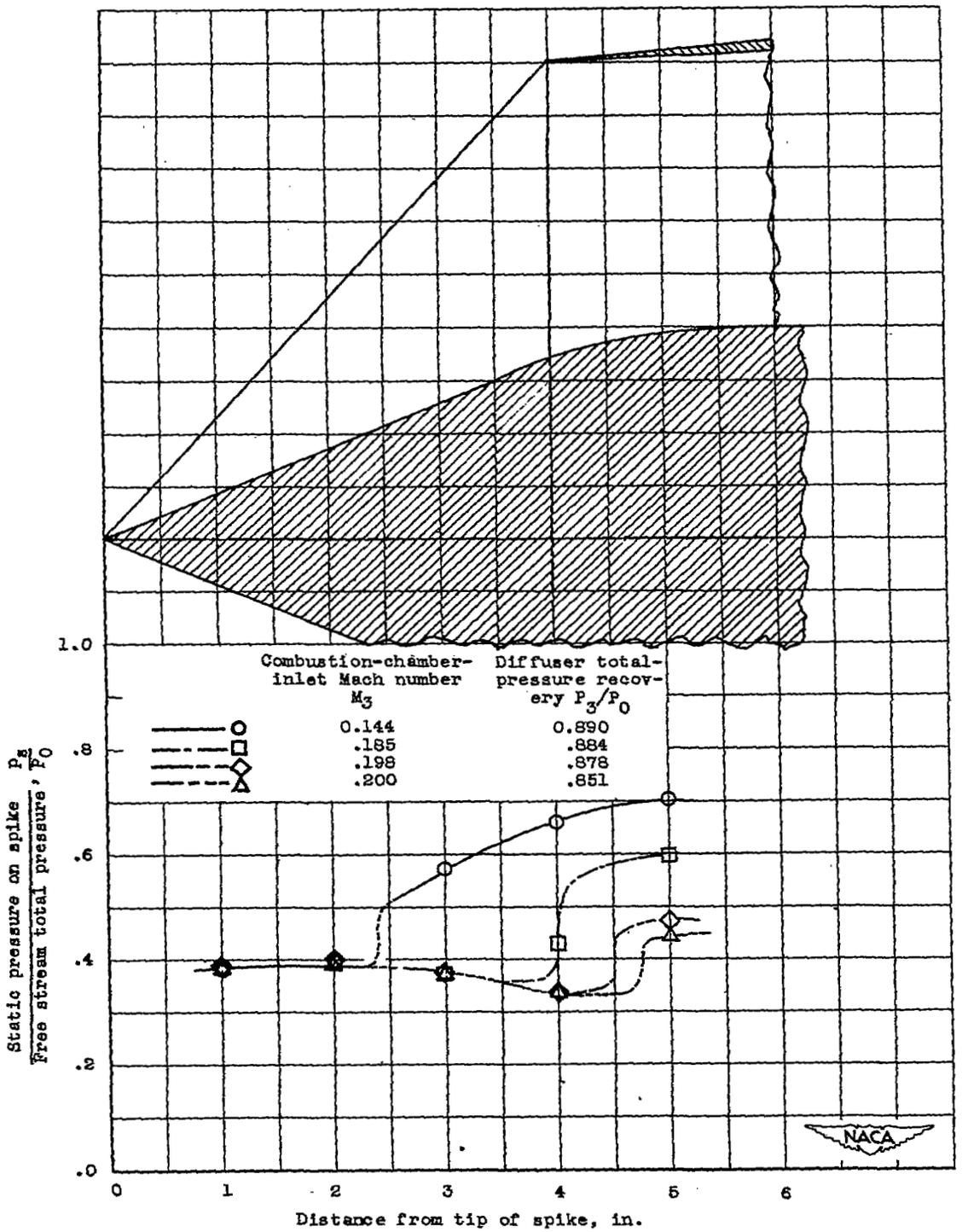

Figure 19. - Typical spike static-pressure distributions at free-stream Mach number M_0 of 1.73.

[redacted]

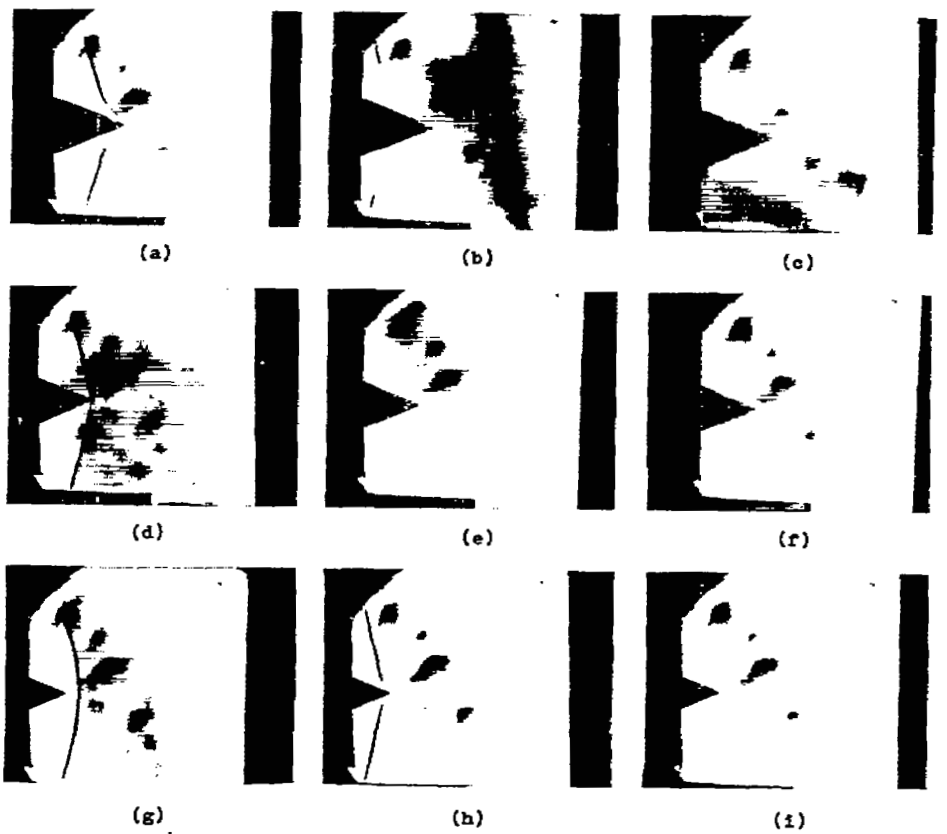

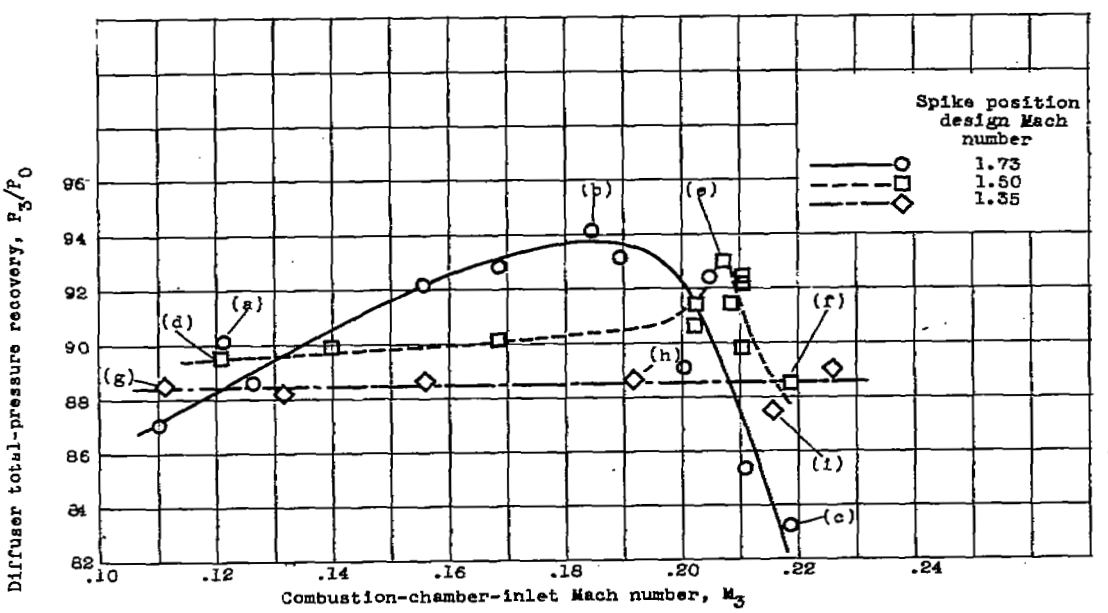

Figure 20. - Effect of tip projection on diffuser total-pressure recovery at free-stream Mach number M_0, 1.50.